DOI: 10.1002/ejic.201100470

# Chiral Diamine Bis(phenolate) $Ti^{IV}$ and $Zr^{IV}$ Complexes – Synthesis, Structures and Reactivity

**Sónia Barroso,[a] Pedro Adão,[a] M. Teresa Duarte,[a] Auke Meetsma,[b] João Costa Pessoa,[a] Marco W. Bouwkamp,[b] and Ana M. Martins*[a]**

**Keywords:** Titanium / Zirconium / Chiral ligands / Polymerization

Neutral and cationic titanium and zirconium diamine bis(phenolate) complexes supported by chiral ligands $L^1$ and $L^2$ are described [$L^1$ = (*R*)-6,6′-{1-(dimethylamino)propan-2-ylazanediyl}bis(methylene)-bis(2,4-di-*tert*-butylphenolate); $L^2$ = (*S*)-6,6′-{(1-ethylpyrrolidin-2-yl)methylazanediyl}bis-(methylene)-bis(2,4-di-*tert*-butylphenolate)]. Complexes [$TiL(OiPr)_2$] [L = $L^1$ (**1**), $L^2$ (**2**)], [$TiL^2X(OiPr)$] [X = Cl (**3**), $CH_2Ph$ (**4**)], [$TiL^1(CH_2Ph)_2$] (**5**), [$ZrLCl_2$] [L = $L^1$ (**6**), $L^2$ (**7**)] and [$ZrL(CH_2Ph)_2$] [L = $L^1$ (**8**), $L^2$ (**9**)] are $C_1$-symmetric species readily prepared in moderate to high yields. Cationic compounds were obtained from complexes **5**, **8** and **9** through reactions with $B(C_6F_5)_3$. The monocationic species reveal the $\eta^2$-binding character of the benzyl groups and noncoordinated $[B(C_6F_5)_3(CH_2Ph)]^-$. Complexes **5**–**9** were tested in the polymerization of ethylene and propylene upon activation with modified methylaluminoxane (MMAO), $B(C_6F_5)_3$ or $[NHMe_2Ph]^+$ as cocatalysts. The [$ZrL^1Cl_2$]/MMAO and [$ZrL^1(CH_2Ph)_2$]/$B(C_6F_5)_3$ systems revealed high activities in the polymerization of propylene ($2.1 \times 10^3$ and $1.5 \times 10^3$ $g_{pol}\,mmol_{cat}^{-1}\,h^{-1}$, respectively), leading to atatic polypropylene, whereas the titanium complexes showed no activity.

## Introduction

There has been a growing interest in the development of postmetallocene single-site transition metal catalysts for alkene polymerization in order to achieve control over the stereochemistry and molecular weight of the polymers.[1] In recent years, group 4 transition metal complexes supported by chelating ligands containing nitrogen and/or oxygen coordinating sites have received considerable attention as active catalysts for olefin polymerization.[1,2] Aryloxide ligands are particularly attractive since they form strong metal–oxygen bonds with electropositive group 4 metals, which are expected to stabilize the resulting complexes.

Group 4 amine bis(phenolate) metal complexes are effective catalysts for 1-hexene,[3] 4-methylpentene,[4] vinylcyclohexane[4] and propylene polymerization,[5] and for ethylene/1-hexene copolymerization.[6] Evaluation of structural modifications in the activity of titanium and zirconium diamine bis(phenolate) catalysts has shown the importance of the bulkiness and electronic properties of the phenolate substituents in 1-hexene polymerization. When activated with $B(C_6F_5)_3$, [$TiL^{Cl}(CH_2Ph)_2$] (Figure 1) was found to be highly active in 1-hexene polymerization giving the highest molecular weight poly(1-hexene) ever prepared at room temperature.[3h] In addition, the presence of an extra donor on the sidearm proved to be crucial for the stabilization of active catalytic species and it has been found to suppress chain transfer reactions.[3a,3b] Dibenzyltitanium and zirconium diamine bis(phenolate) complexes [$ML^{tBu}(CH_2Ph)_2$] (M = Ti, Zr, Figure 1), featuring a nitrogen donor on a sidearm, led to exceptionally high activities in the polymerization of 1-hexene and, in the case of titanium, to living polymerization.[3a,3b] The diamine bis(phenolate) zirconium complex [$ZrL^{tBu}(CH_2Ph)_2$] and its dichloride analogue

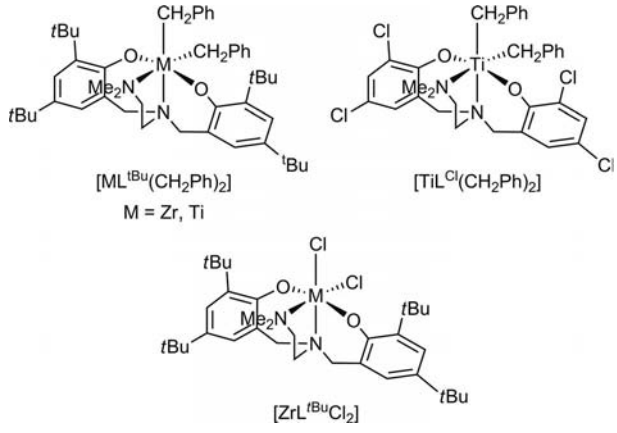


Figure 1. Diamine bis(phenolate) $Ti^{IV}$ and $Zr^{IV}$ complexes active in α-olefin polymerization.

[a] Centro de Química Estrutural, Instituto Superior Técnico, Universidade Técnica de Lisboa,
Av. Rovisco Pais, 1049-001 Lisboa, Portugal
E-mail: ana.martins@ist.utl.pt
[b] Molecular Inorganic Chemistry Group, Stratingh Institute for Chemistry, University of Groningen,
Nijenborgh 4, 9747 AG Groningen, The Netherlands

Supporting information for this article is available on the WWW under http://dx.doi.org/10.1002/ejic.201100470.

  

[$ZrL^{tBu}Cl_2$] (Figure 1) were found to be active propylene polymerization catalysts, upon activation with MAO, leading to high molecular weight, atactic polypropylene.[5]

In view of these results, chiral derivatives of titanium and zirconium diamine bis(phenolate) complexes could be good candidates for the stereoselective polymerization of α-olefins. In fact, Kol and coworkers have recently reported a variety of chiral dianionic ligands of the type [$N_2O_2$] and their corresponding zirconium and titanium complexes for the stereoselective polymerization of α-olefins.[7] However, the only example of a chiral tripodal diamine bis(phenolate) complex reported to date is a molybdenum compound and no catalytic applications have been described.[8]

As part of our research with diamine bis(phenolate) complexes of group 3, 4 and 5 metals[9] we undertook the preparation of chiral tripodal diamine bis(phenol) ligand precursors. Attempts to introduce chirality in the benzylic methylene protons were hampered by the formation of 1,3-benzoxazines.[10] In view of these results we decided to adopt a different strategy and introduce chirality in the carbon chain of the ethylenediamine sidearm (**$H_2L^1$** in Figure 2).[9b] Herein we describe a new chiral diamine bis(phenolate) ligand precursor displaying a ethylpyrrolidine moiety in the sidearm (**$H_2L^2$** in Figure 2) together with neutral and cationic titanium and zirconium complexes supported by these two chiral ligands. The results obtained with these complexes as ethylene and propylene polymerization catalysts are also included.

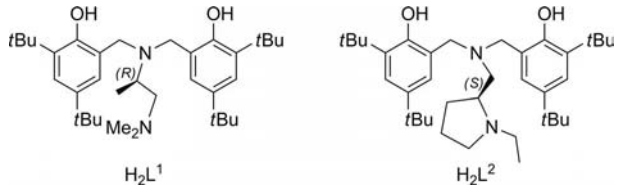


Figure 2. Chiral diamine bis(phenol) ligand precursors employed in this work.

## Results and Discussion

### Synthesis and Characterization of the Ligands and Neutral Complexes

Chiral ligand precursor **$H_2L^2$** (Figure 2), was prepared by a single-step Mannich condensation reaction of a substituted phenol, formaldehyde and an optically pure diamine, (*S*)-(1-ethylpyrrolidin-2-yl)methanamine, following reported procedures.[11] The $^1$H NMR spectrum of **$H_2L^2$** displays only two sets of resonances for the *tert*-butyl groups and for the aromatic protons. However, the resonances assigned to the diamine moiety and the benzylic protons are consistent with a $C_1$-symmetric compound. Thus, the benzylic protons are diastereotopic, appearing as an AB system and all the resonances assigned to the diamine moiety are nonequivalent.

Scheme 1 shows the reactions performed to prepare the new chiral titanium complexes. [$TiL^1(OiPr)_2$] (**1**) and [$TiL^2(OiPr)_2$] (**2**) were obtained as yellow crystalline solids, in good yields, by treating the ligand precursors **$H_2L^1$** and **$H_2L^2$**, respectively, with $Ti(OiPr)_4$ in a 1:1 ratio. The compounds are stable to hydrolysis and do not show any sign of decomposition after several days in air. The $^1$H NMR spectra of **1** and **2** feature two different isopropoxide groups and distinct resonances for the aromatic and aliphatic protons of the ancillary ligands pointing to rigid $C_1$-symmetric chelates on the NMR time scale.

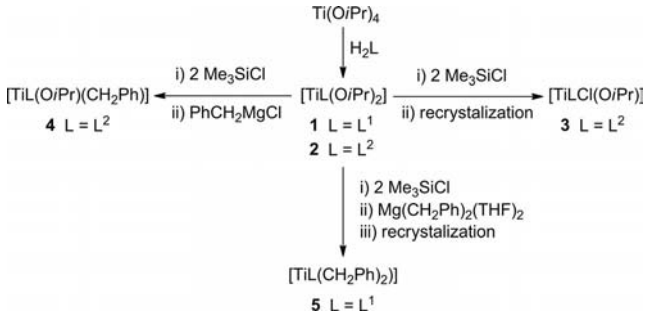


Scheme 1. Synthesis of titanium complexes.

The chirality of **1** and **2** was further confirmed by the CD spectra of THF solutions of both compounds (Figure 3). Although the diamine sidearm moiety is different in the two complexes, the CD spectra of **1** and **2** show that the bands in the range close to 280 nm are nearly mirror images of each other.[12] This is probably due to the similarity between the skeletons of $L^1$ and $L^2$ and the opposite configurations of their chiral carbon atoms (*R* in $L^1$ and *S* in $L^2$). Moreover, the CD spectrum of **2** is more intense than that of **1**, which may be related to the existence of an extra source of chirality upon coordination of the ethylpyrrolidine heterocycle of $L^2$.[13]

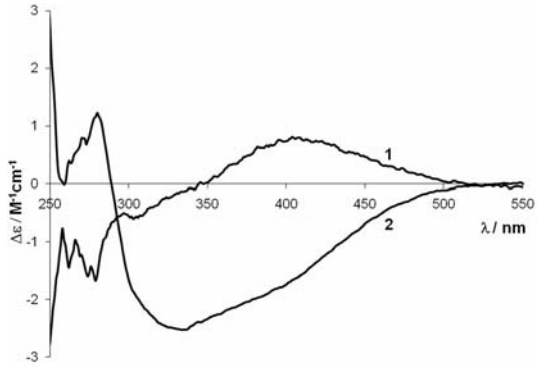


Figure 3. CD spectra of **1** and **2** in THF.

The reaction of M–OR groups with $Me_3SiCl$ is a known procedure for the replacement of alkoxide by chloride ligands as a result of the formation of strong silicon–oxygen bonds.[3a,3d] Aiming to prepare [$TiL^2Cl_2$], **2** was treated with 2 equiv. of $Me_3SiCl$ in dichloromethane. The NMR spectrum of the crude product revealed a complex mixture. Nevertheless, crystals of [$TiL^2Cl(OiPr)$] (**3**) suitable for X-ray diffraction were obtained by recrystallization of the mixture from toluene.

  

Sequential addition of $Me_3SiCl$ and $PhCH_2MgCl$ to a solution of **2** led to [$TiL^2(OiPr)(CH_2Ph)$] (**4**), which was isolated in 70% yield. The NMR spectrum of **4** is consistent with a $C_1$-symmetric species. The two benzylic methylene protons of $L^2$ appear as two AX systems giving rise to four doublets [$\delta$ = 3.85 and 2.84 ppm ($^2J_{HH}$ = 14.5 Hz); $\delta$ = 3.78 and 3.10 ppm ($^2J_{HH}$ = 13.4 Hz)], whereas the methylene protons of the benzyl ligand appear as one AB system [$\delta$ = 3.01 and 3.92 ppm ($^2J_{HH}$ = 8.7 Hz)]. A NOESY experiment pointed out a spatial correlation between the isopropoxide group and the *ortho*-*t*Bu groups attesting its coordination *trans* to the tripodal nitrogen. In addition, the NOESY spectrum shows spatial correlations between one of the *ortho*-*t*Bu groups and the protons of the methyl group of the ethylpyrrolidine moiety attesting for its static coordination to the metal on the NMR time scale. As a result the epimerization of this chiral centre in solution is blocked.

The reaction of **1** with $Me_3SiCl$ followed by the addition of $Mg(CH_2Ph)_2(THF)_2$ led, upon recrystallization from cold pentane, to the isolation of the dibenzyl complex [$TiL^1(CH_2Ph)_2$] (**5**). The $^1H$ NMR spectrum of **5** indicates the formation of a rigid $C_1$-symmetric species. The benzylic methylene protons of $L^1$ are observed as two AB systems, whereas the methylene protons of the benzyl ligands appear as two AX systems. The NMR spectrum is comparable to that previously published for the nonchiral analogue of **5**, [$TiL^{tBu}(CH_2Ph)_2$].[3a,3d] Complex **5** is thermally unstable in solution at room temperature but can be kept in the solid state at –37 °C for several weeks. All attempts to obtain crystals of **5** suitable for X-ray diffraction were unsuccessful.

The reactions performed for the preparation of the new chiral zirconium complexes are shown in Scheme 2. Upon protonolysis of $Zr(CH_2SiMe_3)_2Cl_2(Et_2O)_2$ with the neutral ligand precursors $\mathbf{H_2L^1}$ and $\mathbf{H_2L^2}$ in THF, $SiMe_4$ elimination was observed affording [$ZrL^1Cl_2$] (**6**) and [$ZrL^2Cl_2$] (**7**) in 48 and 16% isolated yield, respectively. The low yields obtained in these reactions are surprising since this procedure is a known entry to the chemistry of zirconium supported by a variety of ligands.[14] In view of this, an alternative method, consisting of the formation of [$ZrL^1(NMe)_2$] and [$ZrL^2(NMe)_2$] intermediates, was attempted. Thus, the reactions of $\mathbf{H_2L^1}$ and $\mathbf{H_2L^2}$ with $Zr(NMe_2)_4$ followed by in situ addition of excess $Me_3SiCl$ led to the isolation of complexes **6** and **7** in 68 and 57% yield, respectively, as light yellow solids. The $^1H$ NMR spectrum of **6** is consistent with a $C_1$-symmetric species displaying two AX spin systems for the benzylic methylene protons of the ligand. The coordination of the $NMe_2$ moiety was confirmed by a NOESY experiment. The $^1H$ NMR spectrum of **7** is consistent with the presence of two isomers of $C_1$ symmetry. The NOESY experiment has shown that there is no dynamic exchange between them. Although many resonances of the minor species are overlapped by the resonances of the major one, the AX spin systems are appreciably different due to the benzylic methylene protons, which is possibly related to ring current effects caused by different locations of these nuclei in relation to the phenolate rings. The two isomers might result either from *trans*/*cis*-phenolate coordination or from diastereomers associated with the chirality of the N2 nitrogen upon bonding to the zirconium, as shown in Figure 4. Isomers of *trans*/*cis*-phenolate coordination have been reported for [$ZrL^{tBu}Cl_2$], which also has a diamine bis(phenolate) donor set bearing a pyridine donor on the side-arm.[14b] However, if *trans*/*cis*-phenolate coordination is assumed for **7**, three different types of isomers would be expected, as shown in Scheme 3. If the two possible configurations, *R*/*S*, resulting from the coordination of N2 are also considered, six diastereoisomers might be expected. The two isomers observed in the $^1H$ NMR spectrum of **7** are tentatively assigned to *trans*-phenolate species with *S* and *R* configuration at N2 in accordance with the geometry observed for compounds **1**–**6**.

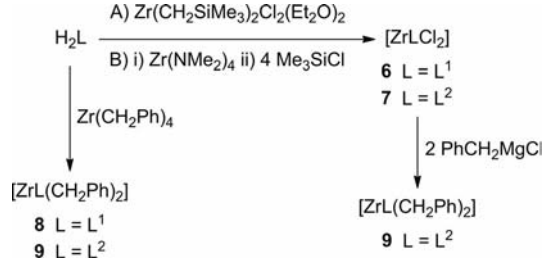


Scheme 2. Synthesis of zirconium complexes.

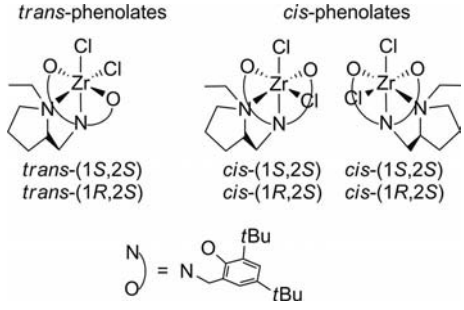


Figure 4. Possible isomers of **7**.

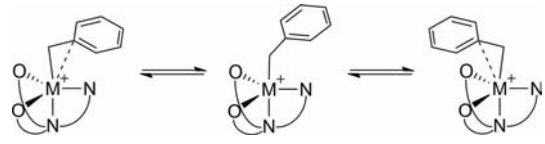

Scheme 3.

The chirality of **6** and **7** was further confirmed by the CD spectra of THF solutions of the complexes (Figure 5). No bands are observed in the visible region of the CD spectra due to the absence of charge transfer bands in that region, also reflected in the light colour of the complexes (pale yellow). As observed for **1** and **2**, the CD spectrum of **6** is more intense than that of **7**, due to the additional chiral centre.[15]

  

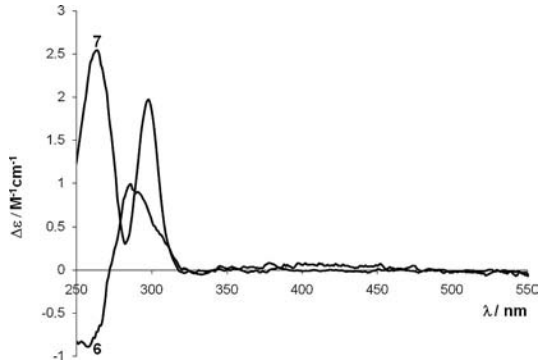


Figure 5. CD spectra of **6** and **7** in THF.

Compounds $[ZrL^1(CH_2Ph)_2]$ (**8**) and $[ZrL^2(CH_2Ph)_2]$ (**9**) were obtained by single-step metathesis reactions between tetrabenzylzirconium and the ligand precursors. Surprisingly, according to $^1H$ NMR spectroscopic data, only one isomer was obtained for **9**, suggesting that formation of two isomers observed for **7** is blocked by the steric bulk of the benzyl group. This assumption was confirmed by the reaction of **7** (mixture of isomers) with 2 equiv. of $PhCH_2MgCl$ that led to the formation of one isomer of **9** in 59% isolated yield. The $^1H$ and $^{13}C$ NMR spectra of **8** and **9** are consistent with $C_1$-symmetric species. The two dibenzyl complexes show characteristic AB systems for the diastereotopic methylene protons of the benzyl ligands in their $^1H$ NMR spectra ($\delta$ = 2.55–2.96 ppm). In the $^{13}C$ NMR spectra the Zr*C*$H_2$Ph methylene group is found in the range $\delta$ = 66–70 ppm with small $^1J_{CH}$ (112–124 Hz). The latter value and the observation of downfield resonances for the *ipso*-carbons suggest $\eta^1$-coordination of the benzyl ligands.[15] For both complexes, the NOESY spectra show spatial correlations that confirm the coordination of the ethylpyrrolidine and dimethylamine nitrogen atoms to the metal centre and *trans* configuration of the phenolate groups. The tripodal ligand forces the two benzyl ligands to be mutually *cis*.

### Generation and Characterization of Cationic Species

The reactions of tris(pentafluorophenyl)borane with **5**, **8** and **9** proceed rapidly and quantitatively at room temperature in [$D_5$]bromobenzene, through the abstraction of one benzyl group and formation of the corresponding cationic species as shown in Scheme 4. In solution, $[ZrL^1(CH_2Ph)_2][PhCH_2B(C_6F_5)_3]$ (**11**) is stable for several days at room temperature, whereas $[TiL^1(CH_2Ph)_2][PhCH_2B(C_6F_5)_3]$ (**10**) decomposes gradually at room temperature over one or two days and is only stable at –35 °C. $[ZrL^2(CH_2Ph)_2][PhCH_2B(C_6F_5)_3]$ (**12**) is unstable and decomposes over a couple of hours even at low temperatures. The high instability of the titanium vs. the zirconium complexes follows the trend observed for first row metal organometallic compounds and is related to weaker metal–ligand bonds.[16] The lower stability of **12** is likely associated with the high steric bulk of the amine sidearm of $L^2$ and the presence of β-H atoms in the ethylpyrrolidine moiety that may provide β-H elimination as an accessible decomposition pathway.

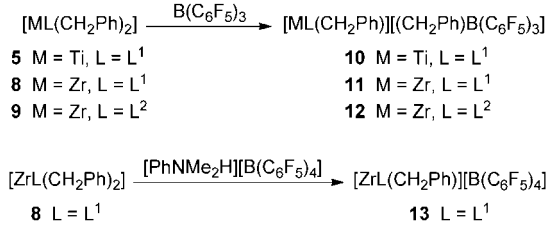


Scheme 4. Generation of the cationic species.

The new complexes were characterised by $^1H$, $^{13}C$ and $^{19}F$ NMR spectra as monocationic species with a noncoordinated $[PhCH_2B(C_6F_5)_3]^-$ anion.[15] The $^1H$ and $^{13}C$ NMR spectra of **10**, **11** and **12** are consistent with $C_1$-symmetric species resembling their neutral precursors. The resonances corresponding to the M*C*$H_2$Ph methylene protons show up as broad singlets in the $^1H$ NMR spectra of the three complexes indicating that the rotation of the benzyl group is constrained.

Relevant chemical shifts for the neutral precursors **5**, **8** and **9** and the corresponding cationic species **10**, **11** and **12** are listed in Table 1. The assessment of the benzyl coordination mode by NMR is often obscured by fluxional processes. However, in static systems $\eta^2$-benzyl ligands in cationic species are usually characterized by downfield-shifted methylene proton resonances and highfield shifts for the *ipso* and the methylene carbon signals when compared to the neutral precursors. A high $^1J_{CH}$ for the methylene group (> 130 Hz) is also an indication of $\eta^2$-benzyl coordination.[17] The upfield shift (> 29 ppm) of the $TiCH_2Ph$ carbon resonance in the $^{13}C$ NMR spectrum of **10**, the high $^1J_{CH}$ value for Zr*C*$H_2$Ph (139 Hz) and the upfield shift of the *ipso* carbon in the $^{13}C$ NMR spectrum of **11** and the upfield shift of the *ipso* carbon resonance in the $^{13}C$ NMR spectrum of **12** are suggestive of $\eta^2$-benzyl coordination to the metal. Although no downfield shift of methylene proton resonances was observed for the cationic species, it is important to mention that these experiments were run at room temperature and that fluxional processes occurring in these conditions may obscure the identification of all criteria. The broad resonances due to the benzyl methylene protons are

Table 1. Selected $^1H$ and $^{13}C$ NMR spectroscopic data for compounds **5** and **8**–**12**.

| | $^1H$ NMR ($\delta$, ppm) M*CH*$_2$ [$^2J_{HH}$, Hz] | $^{13}C$ NMR ($\delta$, ppm) M*C*H$_2$Ph [$^1J_{CH}$, Hz] | $C_{ipso}$ MCH$_2$*Ph* |
|---|---|---|---|
| **5** | 3.56 and 3.34 [8.4]; | 98.6, | 155.2, |
| | 3.26 and 2.79 [9.5] | 85.1 | 148.2 |
| **10** | 3.25, br. | 55.6 | 147.4 |
| **8** | 2.79 and 2.67; | 68.6 [123], | 150.2, |
| | 2.67 and 2.55 [9.8] | 66.6 [121] | 148.0 |
| **11** | 2.94, br. | 72.6 [139] | 131.6 |
| **9** | 2.96 and 2.79; | 69.1 [124], | 148.9, |
| | 2.86 and 2.79 | 68.3 [112] | 148.6 |
| **12** | 2.55, br. | 68.8 | 135.8 |

  

an indication that equilibrium between two $\eta^2$-benzyl isomers takes place in solution as shown in Scheme 3.

The reaction of **8** with $[PhNMe_2H][B(C_6F_5)_4]$ in $[D_5]$bromobenzene leads to $[ZrL^2(CH_2Ph)][B(C_6F_5)_4]$ (**13**) with the release of toluene and $PhNMe_2$ (Scheme 4). The $^1H$ and $^{13}C$ NMR spectra of **13** indicate a cationic species similar to **11**, and the $^{19}F$ NMR spectrum confirms the presence of the $[B(C_6F_5)_4]^-$ anion.

## Catalytic Studies – Ethylene and Propylene Polymerization

The chiral titanium and zirconium complexes were screened for their potential application as catalyst precursors in ethylene and propylene polymerization and the results are presented in Table 2. The activities are based on the observed productivity over the 30 min run time extrapolated to 1 h and they do not take into account possible differences in activity profiles for the various catalysts over the run time. These values are to be used as relative measures of catalyst efficiency rather than absolute activities. All polymers obtained were analysed by high-temperature gel permeation chromatography (HT-GPC).

Upon activation with MMAO, **6** and **7** exhibit low activities[18] in the polymerization of ethylene. Molecular weight analysis of the resulting polymers show narrow polydispersity (PDI = 1.4) for the polyethylene (PE) obtained from **6**, whereas a very wide PDI was obtained with **7**. In the polymerization of propylene, **6** was found to be highly active, with an activity of $2.1 \times 10^3$ $g_{pol}mmol_{cat}^{-1}h^{-1}$, whereas **7** was inactive.

Complex **8**, activated with $B(C_6F_5)_3$ and in the presence of the scavenger tri(isobutyl)aluminoxane (TIBAO), gave the highest activities for the polymerization of ethylene and propylene. These reactions are highly exothermic and are accompanied by heating of the mixture. Complex **9** was inactive in the same conditions, which is possibly related to the instability of **12** discussed above. Complex **8** led to polypropylene (PP) with a polymodal distribution and low molecular weight ($7.4 \times 10^3$ $g\,mol^{-1}$), contrasting with its nonchiral analogue $[ZrL^{tBu}(CH_2Ph)_2]$, which was found to be active in the polymerization of propylene, upon activation with MAO, yielding PP with a high molecular weight ($M_w$ = $3.6 \times 10^5$ $g\,mol^{-1}$) and a narrow PDI of 1.8.[5] $[ZrL^{tBu}(CH_2Ph)_2]$ was also shown to be highly reactive in the polymerization of 1-hexene.[5] Therefore, the performance of **8** was also tested in the polymerization of 1-hexene but it showed no activity.

The mixture of **5** and $B(C_6F_5)_3$ was found to be inactive in the polymerization of ethylene and propylene, even in the presence of a scavenger. This result contrasts with those published for the nonchiral analogue of **5**, $[TiL^{tBu}(CH_2Ph)_2]$, which was found to lead to living polymerization of 1-hexene.[3a]

To investigate the influence of the cocatalyst, $[PhNMe_2H][B(C_6F_5)_4]$ was also used to activate **8** in the presence of TIBAO. Under these conditions, the activity of **8** was lower for the polymerization of ethylene and higher for the polymerization of propylene in comparison to the activities obtained using $[B(C_6F_5)_3]$. However, these small differences were not significant.

Table 2. Data for ethylene, propylene and 1-hexene polymerization.[a]

| Precatalyst | Activator (equiv.) | Scavenger (equiv.) | $m_{pol}$ [g] | Activity[b] | $M_w$ [$g\,mol^{-1}$] | $M_n$ [$g\,mol^{-1}$] | PDI ($M_w/M_n$) |
|---|---|---|---|---|---|---|---|
| Ethylene polymerization[c] | | | | | | | |
| **6** | MMAO (200) | | 0.090 | $4 \times 10^1$ | $1.1 \times 10^3$ | $8.1 \times 10^2$ | 1.4 |
| **7** | MMAO (200) | | 0.017 | 7 | $6.9 \times 10^5$ | $2.9 \times 10^3$ | 240.9 |
| **8** | $B(C_6F_5)_3$ (1) | | traces | | | | |
| **9** | $B(C_6F_5)_3$ (1) | | traces | | | | |
| **5** | $B(C_6F_5)_3$ (1) | TIBAO (20) | traces | | | | |
| **8** | $B(C_6F_5)_3$ (1) | TIBAO (20) | 1.395 | $5.6 \times 10^2$ | $2.1 \times 10^4$ | $5.4 \times 10^3$ | 3.8 |
| **9** | $B(C_6F_5)_3$ (1) | TIBAO (20) | traces | | | | |
| **8** | $[NHMe_2Ph][B(C_6F_5)_4]$ (1) | TIBAO (20) | 0.993 | $3.8 \times 10^2$ | $3.7 \times 10^4$ | $1.1 \times 10^4$ | 3.4 |
| Propylene polymerization[c] | | | | | | | |
| **6** | MMAO (200) | | 5.314 | $2.1 \times 10^3$ | $7.5 \times 10^3$ | $2.1 \times 10^3$ | 3.6 |
| **7** | MMAO (200) | | traces | | | | |
| **8** | $B(C_6F_5)_3$ (1) | | traces | | | | |
| **9** | $B(C_6F_5)_3$ (1) | | traces | | | | |
| **5** | $B(C_6F_5)_3$ (1) | TIBAO (20) | traces | | | | |
| **8** | $B(C_6F_5)_3$ (1) | TIBAO (20) | 3.665 | $1.5 \times 10^3$ | $7.4 \times 10^3$ | $1.3 \times 10^3$ | 5.8 |
| **9** | $B(C_6F_5)_3$ (1) | TIBAO (20) | traces | | | | |
| **8** | $[NHMe_2Ph][B(C_6F_5)_4]$ (1) | TIBAO (20) | 7.454 | $3.0 \times 10^3$ | $8.0 \times 10^3$ | $1.2 \times 10^3$ | 6.5 |
| 1-Hexene polymerization[d] | | | | | | | |
| **6** | MMAO (200) | | 1.343 | $5.4 \times 10^2$ | $4.5 \times 10^3$ | $2.1 \times 10^3$ | 2.2 |
| **8** | $B(C_6F_5)_3$ (1) | | n.d. | | | | |

[a] Precatalyst: 5 μmol; $t$ = 30 min. [b] $g_{pol}mmol_{cat}^{-1}h^{-1}$. [c] Monomer pressure: 5 bar. [d] Monomer: 9 mL (6.06 g).

  

Despite the chirality of the catalyst precursors no enantioselectivity was achieved since all PP samples obtained were atactic according to $^{13}C$ NMR spectra.

Aiming to obtain information about the catalytic reactions, one equivalent of ethylene was added, at ambient temperature, to a NMR tube containing a [$D_5$]bromobenzene solution of **11**. Upon stirring for a few minutes, the $^1H$ NMR spectrum indicates the presence of **11** and a new $C_1$-symmetric species that seems to present an interaction between the zirconium and ethylene. Indeed, ethylene resonances in the mixture appear as one singlet at $\delta$ = 5.13 ppm in the $^1H$ NMR spectrum and give rise to a signal at $\delta$ = 75.7 in the $^{13}C$ NMR spectrum ($^1H$ $\delta$ = 5.29 ppm, $^{13}C$ $\delta$ = 123.9 ppm for free ethylene).[19] After 24 h stirring no significant changes were observed in the $^1H$ NMR spectrum. Upon addition of excess ethylene (+5 equiv.) the solution becomes slightly turbid and broadening of the NMR signals is observed. The resonances assigned to **11** disappear, indicating that its conversion to new compound(s) is complete. The NMR spectroscopic data did not allow further conclusions but indicate that **11** interacts with ethylene in solution.

### Single-Crystal X-ray Diffraction Studies

Suitable crystals for X-ray diffraction were obtained for $\mathbf{H_2L^1}$, $\mathbf{H_2L^2}$, **3**, **6** and **8**.

$\mathbf{H_2L^1}$ crystallizes in the orthorhombic system, space group *Pbca*, with two symmetry-independent molecules in the asymmetric unit as depicted in Figure 6. $\mathbf{H_2L^2}$ crystallizes in the monoclinic system, space group $P2_1$ with four symmetry-independent molecules in the asymmetric unit as depicted in Figure 7. The configurations adopted by both compounds in the solid state are determined by O–H···N and O–H···O intramolecular hydrogen bond interactions. Selected structural parameters for $\mathbf{H_2L^1}$ and $\mathbf{H_2L^2}$ and a more detailed description are given in the Supporting Information.

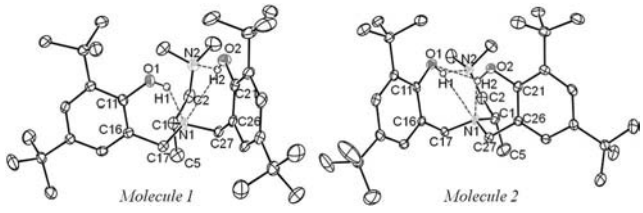


Figure 6. ORTEP diagram of $\mathbf{H_2L^1}$, 40% probability level ellipsoids. Hydrogen atoms are omitted for clarity.

An ORTEP diagram of the molecular structure of **3** is shown in Figure 8 and selected structural parameters are listed in Table 3. The compound crystallizes in the triclinic system, space group *P*1, with one molecule of **3** and one toluene solvate molecule in the asymmetric unit. The titanium centre displays a distorted octahedral geometry with the equatorial plane defined by atoms O1, O2 and N2 of the diamine bis(phenolate) ligand and Cl1, and the axial

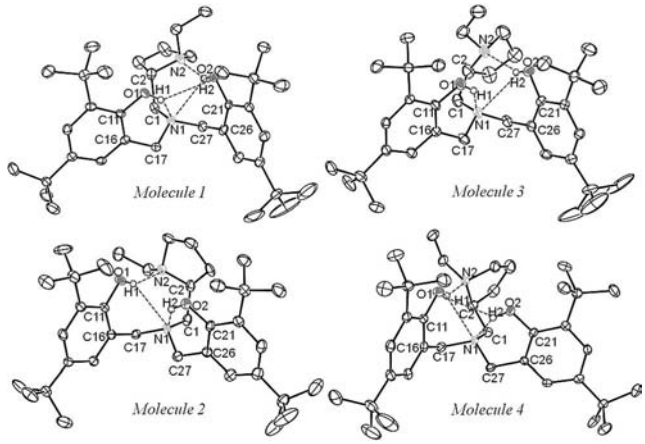


Figure 7. ORTEP diagram of $\mathbf{H_2L^2}$, 40% probability level ellipsoids. Hydrogen atoms are omitted for clarity.

positions are occupied by the tripodal nitrogen N1 and by O3 of the isopropoxide ligand. The titanium atom is slightly displaced from the equatorial plane [0.24(1) Å], in the direction of the isopropoxide ligand. The phenolate groups display *trans* configuration, folding towards the chloride ligand with a narrow dihedral angle of 121(1)° between the planes containing the phenolate rings, reflecting the bulkiness of the heterocyclic amine. The pyrrolidine cycle is coordinated to the metal through the nitrogen atom N2. Chiral atoms N2 and C2 have *S* configuration, and the five-membered metallacycle is defined by Ti1–N1–C1–C2–N2, which displays δ conformation. The least square plane containing the pyrrolidine ring defines a dihedral angle of 72.6(6)° with the equatorial plane and dihedral angles of 24.2(7) and 64.1(8)° with the planes containing the phenolate rings (planes that include C11 and C21, respectively). The relatively short Ti1–O3 bond length [1.79(1) Å] is consistent with a pronounced π-donation from the isopropoxide oxygen atom to the metal. This effect is commonly observed in titanium(IV) alkoxy derivatives[20] and is more pronounced for this type of ligand than for the phenoxide groups, which display Ti–O bond lengths of 1.89(1) Å.

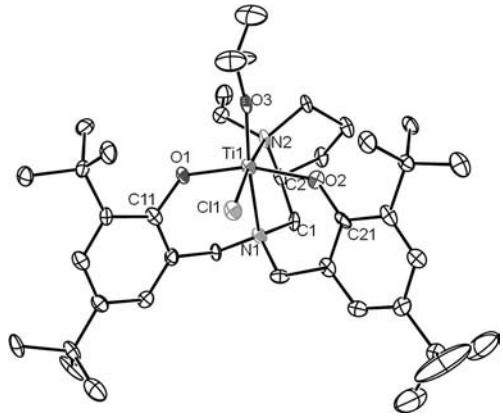

Figure 8. ORTEP diagram of **3**, 40% probability level ellipsoids. Hydrogen atoms are omitted for clarity.

  

Table 3. Selected structural parameters for **3**, **6** and **8**.[a]

| | **3** | **6** | **8** | | **3** | **6** | **8** |
|---|---|---|---|---|---|---|---|
| Distances [Å] | | | | | | | |
| M(1)–O(1) | 1.89(1) | 1.979(5) | 1.996(1) | M(1)–X(1) | 1.79(1) | 2.422(2) | 2.310(2) |
| M(1)–O(2) | 1.89(1) | 1.978(6) | 1.989(2) | M(1)–X(2) | 2.37(0) | 2.441(3) | 2.345(2) |
| M(1)–N(1) | 2.31(1) | 2.393(7) | 2.453(2) | M(1)–C(72) | | | 3.002(2) |
| M(1)–N(2) | 2.32(1) | 2.437(7) | 2.610(2) | M(1)–C(82) | | | 3.314(2) |
| M(1)–equat. plane[b] | 0.244(2) | 0.239(2) | 0.209(2) | | | | |
| Angles [°] | | | | | | | |
| O(1)–M(1)–O(2) | 161.4(4) | 160.8(2) | 160.5(1) | O(2)–M(1)–N(2) | 91.5(4) | 87.8(2) | 87.7(1) |
| O(1)M(1)–N(1) | 83.8(4) | 80.8(2) | 80.8(1) | O(2)–M(1)–X(2) | 86.4(3) | 99.6(2) | 91.7(1) |
| O(1)–M(1)–X(1) | 98.8(4) | 98.6(2) | 98.8(1) | N(1)–M(1)–X(1) | 164.1(4) | 160.7(2) | 149.9(1) |
| O(1)–M(1)–N(2) | 91.2(4) | 87.4(2) | 85.9(1) | N(1)–M(1)–N(2) | 75.7(4) | 74.5(2) | 69.8(1) |
| O(1)–M(1)–X(2) | 87.9(3) | 92.3(2) | 93.2(1) | N(1)–M(1)–X(2) | 95.0(3) | 99.4(2) | 105.8(1) |
| O(2)–M(1)–N(1) | 79.1(4) | 80.0(2) | 79.7(1) | X(1)–M(1)–X(2) | 100.8(3) | 99.9(1) | 104.3(1) |
| O(2)–M(1)–X(1) | 99.6(4) | 99.6(2) | 98.2(1) | N(2)–M(1)–X(2) | 170.7(3) | 173.8(2) | 175.6(1) |
| X(1)–M(1)–N(2) | 88.5(4) | 86.3(2) | 80.1(1) | M(1)–C(71)–C(72) | | | 102.5(1) |
| M(1)–O(1)–C(11) | 130.7(7) | 145.2(5) | 145.3(1) | M(1)–C(81)–C(82) | | | 118.4(1) |
| M(1)–O(2)–C(21) | 135.3(8) | 146.9(5) | 145.7(1) | $\theta$[c] | 120.7(7) | 157.2(3) | 152.7(1) |

[a] M = Ti in **3** and Zr in **6** and **8**; X(1) = O(3) in **3**, Cl(1) in **6** and C(71) in **8**; X(2) = Cl(1) in **3**, Cl(2) in **6** and C(81) in **8**. [b] The equatorial plane is defined by atoms O(1), O(2), N(2) and X(2). [c] $\theta$ is the dihedral angle between the planes containing the phenolate rings.

The molecular structure of complex **6** is depicted in Figure 9 and selected structural parameters are listed in Table 3. The compound crystallizes from toluene in the monoclinic system, space group $P2_1/c$, with one molecule in the asymmetric unit. Compound **6** displays distorted octahedral geometry with the equatorial plane defined by atoms O1, O2, N2 and Cl2, and the axial positions occupied by the tripodal nitrogen N1 and Cl1. The zirconium atom is slightly away from the equatorial plane [0.227(3) Å] in the direction of Cl1. The overall structural parameters of **6** are comparable to the nonchiral analogue $[ZrL^{tBu}Cl_2]$.[5] The structure presents the phenolate groups in *trans* configuration, bending towards the sidearm with a dihedral angle of 157.2(3)° between the planes containing the phenolate rings. Despite the formal absence of a mirror plane in the molecule, the overall ligand core remains quasisymmetrical because the $C_2$ chain of the diamine moiety is twisted to accommodate the extra methyl group away from the phenolate groups, thus nearly bisecting the angle between them.

The molecular structure of **8** is depicted in Figure 10 and selected structural parameters are listed in Table 3. The compound crystallizes from toluene in the monoclinic system, space group $P2_1/c$, with one molecule of **8** and one toluene solvate molecule in the asymmetric unit. The geometry around the zirconium centre is again distorted octahedral with the equatorial plane defined by atoms O1, O2 and N2 of $L^1$ and C81 of one of the benzyl ligands, whereas the axial positions are occupied by the tripodal nitrogen N1 and C71 of the other benzyl ligand. The phenolate groups are mutually *trans*, in accordance with the discussion of the NMR results, and bend towards the dimethylamine sidearm defining a dihedral angle of 152.7(1)°. The zirconium atom is slightly away from the equatorial plane [0.209(2) Å] in the direction of the benzyl ligand. The $NMe_2$ moiety is weakly bonded to the metal as indicated by the long Zr1–N2 bond

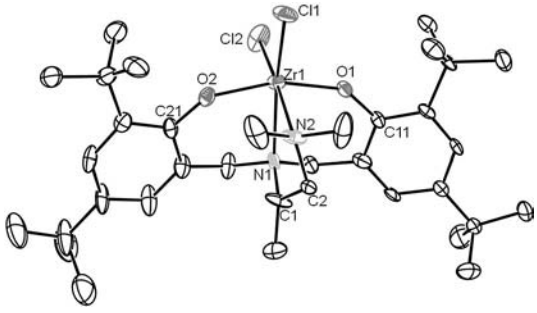


Figure 9. ORTEP diagram of **6**, 40% probability level ellipsoids. Hydrogen atoms and a disordered carbon atom are omitted for clarity.

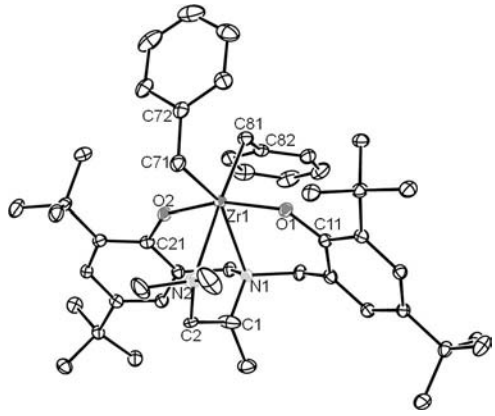


Figure 10. ORTEP diagram of **8**, 40% probability level ellipsoids. Hydrogen atoms and a disordered carbon atom are omitted for clarity.

  

length of 2.610(2) Å. In general the structure of **8** resembles that of **6**. The longer Zr–N bond lengths in **8** may be attributed to a richer metal centre and higher steric bulk caused by the benzyl ligands.

There is a noticeable difference in the bonding mode of the two benzyl ligands in the structure of **8**. The narrower Zr1–C71–C72 angle [102.5(1) vs. 118.4(1)°], as well as the shorter Zr1–C72 distance [3.002(2) vs. 3.314(2) Å] observed in one benzyl group (Figure 10), point to partial $\eta^2$-binding to the Zr.[3c,17]

As shown in Figure 11 the arrangement around the tripodal nitrogen N1 in **3** is helical, whereas the structures of **6** and **8** present a nearly symmetric arrangement of the phenolates that bend towards the sidearm.

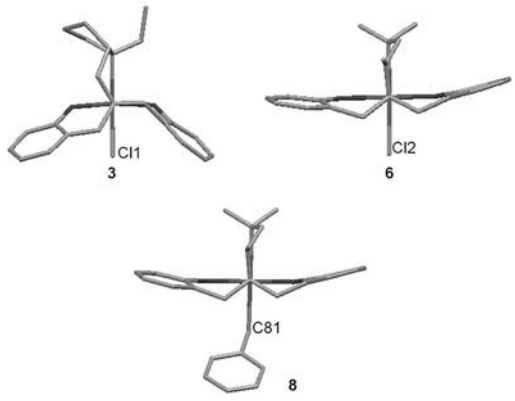


Figure 11. Wireframe diagrams of **3**, **6** and **8** viewed along the N1–M axis (M = Ti in **3**, Zr in **6** and **8**). Groups in *trans* position relative to the tripodal nitrogen (O*i*Pr in **3**, Cl1 in **6** and $CH_2Ph$ in **8**) and the *tert*-butyl groups are omitted for clarity.

The centrosymmetric space groups obtained for the structures of $\mathbf{H_2L^1}$, **6** and **8** indicate that the resolution of the racemic diamine for the preparation of ligand precursor $\mathbf{H_2L^1}$ was not efficient.

## Conclusions

New chiral neutral and cationic diamine bis(phenolate) complexes were prepared and characterized. With the exception of $[TiL(O\mathit{i}Pr)_2]$ [L = $L^1$ (**1**), $L^2$ (**2**)], the titanium compounds are, in general, less stable than the zirconium analogues. The compounds derived from $L^1$ are closely related to their nonchiral analogues concerning their structures and properties. The presence of the methyl group α to the tripodal nitrogen atom does not impose a significant change in the complex structures because the torsion of the sidearm $C_2$ chain releases the steric bulk that results from the presence of the substituent. In general, the compounds supported by $L^2$ are less stable than those bearing $L^1$. This feature is related to the high steric bulk imposed by the ethylpyrrolidine moiety and to the presence of β-H atoms, which may provide an extra decomposition pathway. Furthermore, the presence of two chiral centres [$C_{(S)}$ and $N_{(R/S)}$] upon coordination of $L^2$ gives rise to the formation of one pair of diastereomers for $[ZrL^2Cl_2]$ (**7**). Replacement of the chloride ions by benzyl groups leads to a unique stereoisomer, possibly due to steric constraints.

Compounds **5**, **8** and **9** were used as precursors for cationic complexes formed upon removal of one benzyl ligand. The NMR spectra of these species are indicative of $\eta^2$-benzyl coordination. Assessment of the catalytic properties of the compounds revealed high activities in the polymerization of propylene [2126 and 1466 $g_{pol}mmol_{cat}^{-1}h^{-1}$ for $[ZrL^1Cl_2]$/MMAO and $[ZrL^1(CH_2Ph)_2]/B(C_6F_5)_3$ systems, respectively] yielding atactic polypropylene. Conversely, the titanium complexes showed very low activities in the polymerization of ethylene and propylene.

## Experimental Section

**General:** All preparations and subsequent manipulations of air/moisture sensitive compounds were performed under a nitrogen atmosphere using standard Schlenk line and glovebox techniques. Reagents were purchased from commercial suppliers. $\mathbf{H_2L^1}$, $Zr(CH_2Ph)_4$, $B(C_6F_5)_3$, $Zr(CH_2SiMe_3)_2Cl_2(Et_2O)_2$ and $Mg(CH_2Ph)_2(THF)_2$ were prepared according to literature procedures.[9b,16,21] Solvents (THF, toluene, pentane) were dried by percolation under a nitrogen atmosphere through columns of alumina, molecular sieves, and supported copper oxygen scavenger (BASF R3-11) or by distillation with Na/K alloy (THF, hexane, $Et_2O$, [$D_8$]THF, $C_6D_6$). $C_6D_5Br$ and $CH_2Cl_2$ were dried with $CaH_2$ and distilled under reduced pressure. [$D_8$]Toluene and $CD_2Cl_2$ were dried with molecular sieves (4 Å) and degassed by the freeze-pump-thaw method. NMR spectra were recorded with Varian Inova 500, Varian Gemini VXR 400, Varian VXR 300 and Bruker Advance II+ 300 and 400 MHz (UltraShield Magnet) NMR instruments. $^1H$ and $^{13}C$ chemical shifts ($\delta$) are expressed in ppm relative to $Me_4Si$, whereas $^{19}F$ nucleus was referenced to an external reference capillary with $CF_3COOH$.

### Synthetic Procedures

**$\mathbf{H_2L^2}$:** The diamine used to prepare $\mathbf{H_2L^2}$, (*S*)-(1-ethylpyrrolidin-2-yl)methanamine, was obtained optically active pure from commercial suppliers. A solution of 2,4-di-*tert*-butylphenol (4.13 g, 20.00 mmol), (*S*)-(–)-2-aminomethyl-1-ethylpyrrolidine (1.35 mL, 12.30 mmol) and 36% aqueous formaldehyde (1.65 mL, 22.00 mmol) in methanol (10 mL) was stirred at room temperature for 3 d. The mixture was cooled to –20 °C overnight leading to the formation of a sticky precipitate. The supernatant solution was decanted and the solid was redissolved in MeOH. Upon cooling, the compound precipitated out of solution. The solid was separated by filtration and washed thoroughly with ice cold methanol to give an off-white solid in 30% yield. The compound was further purified by recrystallization from methanol. $^1H$ NMR (300 MHz, $CDCl_3$, 25 °C): $\delta$ = 9.69 (br., 2 H, O*H*), 7.20 (d, $^4J_{HH}$ = 2.2 Hz, 2 H, C*H*-Ar), 6.87 (d, $^4J_{HH}$ = 2.2 Hz, 2 H, C*H*-Ar), 3.87 (d, $^2J_{HH}$ = 13.3 Hz, 2 H, ArC$H_2$N), 3.43 (d, $^2J_{HH}$ = 13.2 Hz, 2 H, ArC$H_2$N), 3.35 (m, 1 H, C$H_2$), 3.04 (m, 1 H, C$H_2$CH$_3$), 2.66 (m, 2 H, C$H_2$, C*H*), 2.48 (m, 1 H, NC$H_2$), 2.25 (m, 2 H, C$H_2$CH$_3$, C$H_2$), 1.90 (m, 1 H, C$H_2$), 1.68 (m, 2 H, C$H_2$), 1.48 (m, 1 H, C$H_2$), 1.39 [s, 18 H, C(C$H_3$)$_3$], 1.27 [s, 18 H, C(C$H_3$)$_3$], 1.20 (t, $^3J_{HH}$ = 7.2 Hz, 3 H, CH$_2$C$H_3$) ppm. $^{13}C\{^1H\}$ NMR (75 MHz, $CDCl_3$, 25 °C): $\delta$ = 153.6, 140.1, 136.0 and 121.8 ($C_{ipso}$-Ar), 124.9 and 123.3 (*C*H-Ar), 64.4 (*C*H), 58.5 (Ar*C*H$_2$N), 54.0 (*C*H$_2$), 53.6 (*C*H$_2$), 50.0 (*C*H$_2$CH$_3$), 34.9 and 34.1 [*C*(CH$_3$)$_3$], 31.7 and 29.6 [C(*C*H$_3$)$_3$], 28.5 (*C*H$_2$), 22.8 (*C*H$_2$), 13.0 (CH$_2$*C*H$_3$) ppm. $C_{37}H_{60}N_2O_2 \cdot 0.1(CH_3OH)$

  

(567.66): calcd. C 78.44, H 10.72, N 4.93; found C 78.36, H 11.21, N 4.94.

**[TiL$^1$(O*i*Pr)$_2$] (1):** A solution of **H$_2$L$^1$** (323 mg, 0.6 mmol) in $Et_2O$ was slowly added to a 1 M solution of Ti(O*i*Pr)$_4$ in $Et_2O$ (0.6 mL, 0.6 mmol) in the same solvent. The solution was stirred for 2 h at room temperature. Evaporation of all the volatiles under reduced pressure led to a yellow solid in 62% yield. $^1$H NMR (300 MHz, $C_6D_6$, 25 °C): $\delta$ = 7.58 (d, $^4J_{HH}$ = 2.5 Hz, 1 H, *p*-C*H*-Ar), 7.56 (d, $^4J_{HH}$ = 2.5 Hz, 1 H, *p*-C*H*-Ar), 7.07 (d, $^4J_{HH}$ = 2.4 Hz, 1 H, *o*-C*H*-Ar), 7.04 (d, $^4J_{HH}$ = 2.5 Hz, 1 H, *o*-C*H*-Ar), 5.25 [sept, $^3J_{HH}$ = 6.1 Hz, 1 H, C*H*(CH$_3$)$_2$], 4.75 [sept, $^3J_{HH}$ = 6.1 Hz, 1 H, C*H*-(CH$_3$)$_2$], 4.66 (d, $^2J_{HH}$ = 13.8 Hz, 1 H, NC*H*$_2$Ar), 3.51 (d, $^2J_{HH}$ = 13.2 Hz, 1 H, NC*H*$_2$Ar), 3.39 (d, $^2J_{HH}$ = 13.2 Hz, 1 H, NC*H*$_2$Ar), 3.29 (d, $^2J_{HH}$ = 13.9 Hz, 1 H, NC*H*$_2$Ar), 3.19 [m, 1 H, NC*H*(CH$_3$)-CH$_2$N], 2.47 [t, 1 H, NCH(CH$_3$)C*H*$_2$N], 2.34 [s, 3 H, N(C*H*$_3$)$_2$], 2.04 [s, 3 H, N(C*H*$_3$)$_2$], 1.79 [s, 9 H, C(C*H*$_3$)$_3$], 1.76 [s, 9 H, C(C*H*$_3$)$_3$], 1.53 [d, $^3J_{HH}$ = 6.1 Hz, 3 H, CH(C*H*$_3$)$_2$], 1.50 [d, $^3J_{HH}$ = 6.1 Hz, 3 H, CH(C*H*$_3$)$_2$], 1.44 [s, 9 H, C(C*H*$_3$)$_3$], 1.41 [s, 9 H, C(C*H*$_3$)$_3$], 1.12 [m, 1 H, NCH(CH$_3$)C*H*$_2$N], 0.99 [d, $^3J_{HH}$ = 6.1 Hz, 3 H, CH(C*H*$_3$)$_2$], 0.88 [d, $^3J_{HH}$ = 6.1 Hz, 3 H, CH(C*H*$_3$)$_2$], 0.59 [d, $^3J_{HH}$ = 6.7 Hz, 3 H, NCH(C*H*$_3$)CH$_2$N] ppm. $^{13}$C{$^1$H} NMR (75 MHz, $C_6D_6$, 25 °C): $\delta$ = 163.4, 160.1, 139.5, 139.2, 136.2, 134.7, 125.9 and 124.4 ($C_{ipso}$-Ar), 124.7 and 124.3 (*C*H-Ar), 77.9 and 77.8 [*C*H(CH$_3$)$_2$], 64.6 [NCH(CH$_3$)*C*H$_2$N], 62.1 and 57.3 (N*C*H$_2$Ar), 53.0 [N*C*H(CH$_3$)CH$_2$N], 51.3 and 50.1 [N(*C*H$_3$)$_2$], 36.1, 35.9 and 34.7 [*C*(CH$_3$)$_3$], 32.5, 32.4, 31.5 and 31.4 [C(*C*H$_3$)$_3$], 27.6, 27.5, 26.7 and 26.5 [CH(*C*H$_3$)$_2$], 8.7 [NCH(*C*H$_3$)CH$_2$N] ppm. $C_{41}H_{70}N_2O_4Ti\cdot 3.5(C_3H_8O)$ (912.61): calcd. C 67.73, H 10.82, N 3.07; found C 67.79, H 11.04, N 2.84.

**[TiL$^2$(O*i*Pr)$_2$] (2):** A solution of **H$_2$L$^2$** (339 mg, 0.6 mmol) in $Et_2O$ was slowly added to a 1 M solution of Ti(O*i*Pr)$_4$ in $Et_2O$ (0.6 mL, 0.6 mmol) in the same solvent. The solution was stirred for 2 h at room temperature. Evaporation of all the volatiles under reduced pressure led to a yellow solid in 64% yield. $^1$H NMR (400 MHz, $C_6D_6$, 25 °C): $\delta$ = 7.58 (d, $^4J_{HH}$ = 2.4 Hz, 1 H, *p*-C*H*-Ar), 7.51 (d, $^4J_{HH}$ = 2.3 Hz, 1 H, *p*-C*H*-Ar), 7.18 (d, $^4J_{HH}$ = 2.5 Hz, 1 H, *o*-C*H*-Ar), 6.69 (d, $^4J_{HH}$ = 2.2 Hz, 1 H, *o*-C*H*-Ar), 5.14 [sept, $^3J_{HH}$ = 6.1 Hz, 1 H, C*H*(CH$_3$)$_2$], 4.90 (d, $^2J_{HH}$ = 14.4 Hz, 1 H, NC*H*$_2$Ar), 4.29 [sept, $^3J_{HH}$ = 6.1 Hz, 1 H, C*H*(CH$_3$)$_2$], 4.10 (m, 1 H, C*H*$_2$), 3.89 (d, $^2J_{HH}$ = 12.3 Hz, 1 H, NC*H*$_2$Ar), 3.29 (m, 2 H, C*H*$_2$CH$_3$), 3.19 (d, $^2J_{HH}$ = 14.6 Hz, 1 H, NC*H*$_2$Ar), 2.96 (m, 1 H, NCH$_2$C*H*), 2.86 (t, $^2J_{HH}$ = 12.4 Hz, 1 H, C*H*$_2$), 2.69 (d, $^2J_{HH}$ = 12.4 Hz, 1 H, NC*H*$_2$Ar), 2.63 (m, 1 H, C*H*$_2$), 1.79 [s, 9 H, C(C*H*$_3$)$_3$], 1.77 [s, 9 H, C(C*H*$_3$)$_3$], 1.51 [d, $^3J_{HH}$ = 3.8 Hz, 3 H, CH(C*H*$_3$)$_2$], 1.49 [d, $^3J_{HH}$ = 3.8 Hz, 3 H, CH(C*H*$_3$)$_2$], 1.47 [s, 9 H, C(C*H*$_3$)$_3$], 1.44 (m, 2 H, C*H*$_2$), 1.38 (m, 1 H, C*H*$_2$), 1.34 [s, 9 H, C(C*H*$_3$)$_3$], 1.20 (m, 1 H, NC*H*$_2$CH), 0.92 (t, $^3J_{HH}$ = 7.2 Hz, 3 H, CH$_2$C*H*$_3$), 0.72 [d, $^3J_{HH}$ = 6.1 Hz, 3 H, CH(C*H*$_3$)$_2$], 0.55 (m, 1 H, NC*H*$_2$CH), 0.48 [d, $^3J_{HH}$ = 6.1 Hz, 3 H, CH(C*H*$_3$)$_2$] ppm. $^{13}$C{$^1$H} NMR (101 MHz, $C_6D_6$, 25 °C): $\delta$ = 164.4, 159.7, 139.6, 139.2, 136.6, 134.5 and 125.0 ($C_{ipso}$-Ar), 124.3, 124.1 and 124.0 (*C*H-Ar), 123.5 ($C_{ipso}$-Ar), 123.0 (*C*H-Ar), 78.0 and 77.9 [*C*H(CH$_3$)$_2$], 63.6 (N*C*H$_2$Ar), 62.9 (NCH$_2$*C*H), 61.8 (N*C*H$_2$Ar), 61.1, 54.7 and 53.4 (*C*H$_2$), 36.1, 35.8, 34.7 and 34.6 [*C*(CH$_3$)$_3$], 32.6, 32.4, 31.3 and 31.3 [C(*C*H$_3$)$_3$], 29.2 (*C*H$_2$), 27.3, 27.2, 26.2 and 25.8 [CH(*C*H$_3$)$_2$], 25.2 (*C*H$_2$), 11.0 (CH$_2$*C*H$_3$) ppm. $C_{43}H_{72}N_2O_4Ti\cdot 2.5(C_3H_8O)$ (878.56): calcd. C 68.99, H 10.55, N 3.19; found C 68.66, H 10.26, N 3.19.

**[TiL$^2$Cl(O*i*Pr)] (3):** A 1 M solution of Si(Me)$_3$Cl in $CH_2Cl_2$ (5.00 mL, 5.00 mmol) was added to a solution of **2** (1.82 g, 2.50 mmol) in $CH_2Cl_2$ and the mixture was stirred for 2 h at room temperature. All the volatiles were removed under reduced pressure to give an orange solid. Analysis of the NMR spectroscopic data revealed a complex mixture of compounds. Orange crystals of **3** were obtained from a toluene solution of the mixture at –37 °C. The small amount of crystals obtained prevented further characterization.

**[TiL$^2$(O*i*Pr)(CH$_2$Ph)] (4):** A 1 M solution of Si(Me)$_3$Cl in $CH_2Cl_2$ (0.42 mL, 0.42 mmol) was added to a solution of **2** (153.1 mg, 0.21 mmol) in $CH_2Cl_2$ and the mixture was stirred for 2 h at room temperature. All the volatiles were removed under reduced pressure. The residue was redissolved in $Et_2O$ and a 1 M solution of PhCH$_2$MgCl in $Et_2O$ (0.42 mL, 0.42 mmol) was added and the mixture was further stirred for 2 h at room temperature. The solution was filtered and the solvent was evaporated under reduced pressure to give a red solid in 70% yield. $^1$H NMR (300 MHz, $C_6D_6$, 25 °C): $\delta$ = 7.64 (s, 1 H, *p*-C*H*-Ar), 7.59 (s, 1 H, *p*-C*H*-Ar), 7.09 (s, 1 H, *o*-C*H*-Ar), 6.96 (m, 2 H, CH$_2$*Ph*), 6.92 (s, 1 H, *o*-C*H*-Ar), 6.83 (d, $^3J_{HH}$ = 7.7 Hz, 2 H, CH$_2$*Ph*), 6.75 (t, $^3J_{HH}$ = 7.2 Hz, 1 H, CH$_2$*Ph*), 5.14 [sept, $^3J_{HH}$ = 6.0 Hz, 1 H, C*H*(CH$_3$)$_2$], 3.85 (d, $^2J_{HH}$ = 14.5 Hz, 1 H, NC*H*$_2$Ar), 3.78 (d, $^2J_{HH}$ = 13.4 Hz, 1 H, NC*H*$_2$Ar), 3.10 (d, $^2J_{HH}$ = 13.4 Hz, 1 H, NC*H*$_2$Ar), 3.01 (d, $^2J_{HH}$ = 8.7 Hz, 1 H, C*H*$_2$Ph), 2.92 (d, $^2J_{HH}$ = 8.7 Hz, 1 H, C*H*$_2$Ph), 2.84 (d, $^2J_{HH}$ = 14.5 Hz, 1 H, NC*H*$_2$Ar), 2.74 (m, 1 H, C*H*$_2$), 2.70 (m, 1 H, C*H*$_2$), 2.60 (m, 1 H, NCH$_2$C*H*), 2.58 (m, 1 H, C*H*$_2$CH$_3$), 2.23 (m, 1 H, C*H*$_2$), 1.98 (m, 1 H, C*H*$_2$CH$_3$), 1.86 [s, 9 H, C(C*H*$_3$)$_3$], 1.82 [s, 9 H, C(C*H*$_3$)$_3$], 1.51 [m, 7 H, C*H*$_2$, CH(C*H*$_3$)$_2$], 1.43 [s, 9 H, C(C*H*$_3$)$_3$], 1.39 [s, 9 H, C(C*H*$_3$)$_3$], 1.14 (m, 1 H, C*H*$_2$), 0.85 (m, 2 H, C*H*$_2$), 0.62 (t, $^3J_{HH}$ = 7.1 Hz, 3 H, CH$_2$C*H*$_3$), 0.30 (m, 1 H, C*H*$_2$) ppm. $^{13}$C{$^1$H} NMR (75 MHz, $C_6D_6$, 25 °C): $\delta$ = 161.5, 159.4, 152.1, 141.2, 140.7, 136.7, 135.6 and 129.7 ($C_{ipso}$-Ar), 128.7, 127.9 and 127.3 (*C*H-Ph), 127.0 and 125.9 ($C_{ipso}$-Ph), 124.9, 124.8, 124.2 and 123.9 (*C*H-Ar), 121.5 (*C*H-Ph), 79.8 [*C*H(CH$_3$)$_2$], 76.1 (*C*H$_2$Ph), 65.5 and 65.1 (N*C*H$_2$Ar), 63.5 (NCH$_2$*C*H), 62.5, 50.8 and 50.1 (*C*H$_2$), 36.3, 36.2 and 34.8 [*C*(CH$_3$)$_3$], 32.5, 32.4, 31.8 and 31.3 [C(*C*H$_3$)$_3$], 27.3 (*C*H$_2$), 26.8 and 26.5 [CH(*C*H$_3$)$_2$], 22.6 (*C*H$_2$), 11.7 (CH$_2$*C*H$_3$) ppm. $C_{48}H_{75}N_2O_3Ti\cdot 1.7(CH_2Cl_2)$ (919.80): calcd. C 64.82, H 8.58, N 3.04; found C 64.85, H 8.48, N 3.04.

**[TiL$^1$(CH$_2$Ph)$_2$] (5):** A 1 M solution of Si(Me)$_3$Cl in $CH_2Cl_2$ (6.00 mL, 6.00 mmol) was added to a solution of **2** (1.76 g, 2.50 mmol) in $CH_2Cl_2$ and the mixture was further stirred for 2 h at room temperature. The solvent was evaporated to dryness and the residue was redissolved in THF and treated with a solution of Mg(CH$_2$Ph)$_2$(THF)$_2$ (0.88 g, 2.50 mmol) in THF. The mixture was stirred at room temperature for 4 h and then evaporated to dryness leading to a residue that was extracted in pentane. After filtration the solution was cooled to –54 °C leading to a microcrystalline dark red solid in 41% yield that was separated by filtration and dried in vacuo. $^1$H NMR (500 MHz, $C_6D_6$, 25 °C): $\delta$ = 7.89 (d, $^3J_{HH}$ = 7.4 Hz, 2 H, CH$_2$*Ph*), 7.74 (d, $^4J_{HH}$ = 2.1 Hz, 1 H, C*H*-Ar), 7.70 (d, $^4J_{HH}$ = 2.1 Hz, 1 H, C*H*-Ar), 7.41 (t, $^3J_{HH}$ = 7.6 Hz, 2 H, CH$_2$*Ph*), 7.00 (m, 4 H, C*H*-Ar, CH$_2$*Ph*), 6.90 (d, $^4J_{HH}$ = 2.1 Hz, 1 H, C*H*-Ar), 6.60 (t, $^3J_{HH}$ = 7.5 Hz, 2 H, CH$_2$*Ph*), 6.48 (t, $^3J_{HH}$ = 7.2 Hz, 1 H, CH$_2$*Ph*), 3.56 (d, $^2J_{HH}$ = 8.4 Hz, 1 H, C*H*$_2$Ph), 3.34 (d, $^2J_{HH}$ = 8.4 Hz, 1 H, C*H*$_2$Ph), 3.26 (d, $^2J_{HH}$ = 9.5 Hz, 1 H, C*H*$_2$Ph), 2.98 (d, $^2J_{HH}$ = 14.1 Hz, 1 H, ArC*H*$_2$N), 2.79 (m, $^2J_{HH}$ = 8.9 Hz, 2 H, C*H*$_2$Ph, ArC*H*$_2$N), 2.63 (d, $^2J_{HH}$ = 14.1 Hz, 1 H, ArC*H*$_2$N), 2.52 [m, 1 H, NC*H*(CH$_3$)CH$_2$N], 2.39 (d, $^2J_{HH}$ = 14.0 Hz, 1 H, ArC*H*$_2$N), 2.19 [s, 18 H, C(C*H*$_3$)$_3$], 2.05 [m, 1 H, NCH(CH$_3$)C*H*$_2$N], 1.85 [s, 3 H, N(C*H*$_3$)$_2$], 1.82 [s, 3 H, N(C*H*$_3$)$_2$], 1.36 [s, 9 H, C(C*H*$_3$)$_3$], 1.35 [s, 9 H, C(C*H*$_3$)$_3$], 0.53 [m, 1 H, NCH(CH$_3$)C*H*$_2$N], 0.51 [d, $^3J_{HH}$ = 6.5 Hz, 3 H, NCH(C*H*$_3$)-CH$_2$N] ppm. $^{13}$C-{$^1$H}NMR (126 MHz, $C_6D_6$, 25 °C): $\delta$ = 161.1 and 160.1 ($C_{ipso}$-Ar), 155.2 and 148.2 ($C_{ipso}$-Ph), 141.6, 141.2, 136.1 and 135.3 ($C_{ipso}$-Ar), 128.8 and 128.6 (CH$_2$*Ph*), 128.5 and 127.0 ($C_{ipso}$-Ar), 126.9, 126.7 and 126.2 (CH$_2$*Ph*), 124.7, 124.4, 124.3 and

  

124.0 (*C*H-Ar), 122.0 and 121.9 ($CH_2$*Ph*), 98.6 and 85.1 (*C*$H_2$Ph), 65.7 [NCH($CH_3$)*C*$H_2$N], 61.0 and 56.8 (Ar*C*$H_2$N), 50.6 [N*C*H($CH_3$)$CH_2$N], 37.9, 36.0, 35.8 and 34.2 [*C*($CH_3$)$_3$], 31.8, 31.7 and 31.3 [C(*C*$H_3$)$_3$], 31.2 [N(*C*$H_3$)$_2$], 31.1 [C(*C*$H_3$)$_3$], 30.8 [N(*C*$H_3$)$_2$], 7.5 [NCH(*C*$H_3$)$CH_2$N] ppm. $C_{49}H_{70}N_2O_2Ti$·0.5($C_4H_8O$) (802.44): calcd. C 76.28, H 9.29, N 3.49; found C 76.31, H 9.37, N 3.33.

**[ZrL$^1$Cl$_2$] (6). Method A:** A solution of **H$_2$L$^1$** (1.35 g, 2.50 mmol) in THF was added to a solution of Zr($CH_2SiMe_3$)$_2$Cl$_2$($Et_2O$)$_2$ (1.12 g, 2.50 mmol) in the same solvent. The mixture was stirred at room temperature for 12 h and a white precipitate appeared. The yellow solution was filtered and the solvents evaporated to dryness under reduced pressure to give a light yellow solid in 48% yield.

**Method B:** A solution of **H$_2$L$^1$** (323 mg, 0.6 mmol) in $Et_2O$ was added to a solution of Zr($NMe_2$)$_4$ (161 mg, 0.6 mmol) in the same solvent. The mixture was stirred at room temperature for 2 h. The yellow solution was evaporated to dryness under reduced pressure. The residue was redissolved in $CH_2Cl_2$ and Si(Me)$_3$Cl 1 M in $CH_2Cl_2$ (2.4 mL, 2.4 mmol) was slowly added to the solution. The mixture was stirred at room temperature for 2 h and the yellow solution was evaporated to dryness under reduced pressure. The residue was washed with *n*-hexane and dried in vacuo to give a light yellow solid in 68% yield. $^1$H NMR (400 MHz, $C_6D_6$, 25 °C): $\delta$ = 7.61 (s, 1 H, C*H*-Ar), 7.55 (s, 1 H, C*H*-Ar), 6.92 (s, 2 H, C*H*-Ar), 4.41 (d, $^2J_{HH}$ = 14.1 Hz, 1 H, ArC$H_2$N), 4.06 (d, $^2J_{HH}$ = 14.3 Hz, 1 H, ArC$H_2$N), 2.95 [m, 3 H, ArC$H_2$N, NC*H*($CH_3$)-$CH_2$N], 2.38 [t, $^2J_{HH}$ = 13.1 Hz, 1 H, NCH($CH_3$)C$H_2$N], 2.09 [s, 3 H, N(C$H_3$)$_2$], 1.71 [s, 18 H, C(C$H_3$)$_3$], 1.69 [s, 3 H, N(C$H_3$)$_2$], 1.39 [s, 9 H, C(C$H_3$)$_3$], 1.37 [s, 9 H, C(C$H_3$)$_3$], 0.75 [d, $^2J_{HH}$ = 13.0 Hz, 1 H, NCH($CH_3$)C$H_2$N], 0.54 [d, $^3J_{HH}$ = 6.6 Hz, 3 H, NCH(C$H_3$)-$CH_2$N] ppm. $^{13}$C-{$^1$H}NMR (101 MHz, $C_6D_6$, 25 °C): $\delta$ = 158.2, 156.9, 142.7, 142.5, 138.0, 136.9, 126.7 and 125.5 ($C_{ipso}$-Ar), 125.5, 125.4, 125.1 and 124.7 (*C*H-Ar), 66.1 [NCH($CH_3$)*C*$H_2$N], 62.5 and 58.1 (Ar*C*$H_2$N), 53.2 [N*C*H($CH_3$)$CH_2$N], 51.7 and 48.2 [N(*C*$H_3$)$_2$], 36.1, 36.0, 34.9 and 34.8 [*C*($CH_3$)$_3$], 32.3, 32.2, 31.4 and 31.0 [C(*C*$H_3$)$_3$], 8.3 [NCH(*C*$H_3$)$CH_2$N] ppm. $C_{35}H_{56}Cl_2N_2O_2Zr$·0.6($CH_2Cl_2$) (749.51): calcd. C 57.02, H 7.69, N 3.74; found C 57.01, H 8.48, N 3.36.

**[ZrL$^2$Cl$_2$] (7). Method A:** A solution of **H$_2$L$^2$** (1.41 g, 2.50 mmol) in THF was added to a solution of Zr($CH_2SiMe_3$)$_2$Cl$_2$($Et_2O$) (1.12 g, 2.50 mmol) in the same solvent. The mixture was stirred at room temperature for 12 h and a white precipitate appeared. The yellow solution was filtered and the solvents evaporated to dryness under reduced pressure to give a light yellow solid; yield 0.28 g, 16%.

**Method B:** A solution of **H$_2$L$^2$** (339 mg, 0.6 mmol) in $Et_2O$ was added to a solution of Zr($NMe_2$)$_4$ (161 mg, 0.6 mmol) in the same solvent. The solution was stirred at room temperature for 2 h. The yellow solution was evaporated to dryness under reduced pressure. The residue was redissolved in $CH_2Cl_2$ and Si(Me)$_3$Cl 1 M in $CH_2Cl_2$ (2.4 mL, 2.4 mmol) was slowly added to the solution. The mixture was stirred at room temperature for 2 h. The yellow solution was evaporated to dryness under reduced pressure. The residue was washed with *n*-hexane and dried in vacuo to give a light yellow solid; yield 250 mg, 57%. The analysis of NMR spectroscopic data revealed a mixture of isomers in variable ratios (from 100:1 to 3:1). *Major isomer*: $^1$H NMR (400 MHz, $C_6D_6$, 25 °C): $\delta$ = 7.60 (s, 1 H, C*H*-Ar), 7.58 (s, 1 H, C*H*-Ar), 7.05 (s, 1 H, C*H*-Ar), 6.94 (s, 1 H, C*H*-Ar), 4.79 (d, $^2J_{HH}$ = 13.8 Hz, 1 H, ArC$H_2$N), 3.95 (d, $^2J_{HH}$ = 13.1 Hz, 1 H, ArC$H_2$N), 3.19 (m, 1 H, C$H_2$$CH_3$), 3.07 (m, 2 H, ArC$H_2$N, C$H_2$), 2.89 (m, 2 H, ArC$H_2$N, C*H*), 2.69 (m, 2 H, C$H_2$), 2.20 (m, 1 H, C$H_2$$CH_3$), 1.74 [s, 18 H, C(C$H_3$)$_3$], 1.53 (m, 1 H, C$H_2$), 1.40 [s, 9 H, C(C$H_3$)$_3$], 1.35 [s, 9 H, C(C$H_3$)$_3$], 0.80 (m, 1 H, C$H_2$), 0.70 (m, 3 H, C$H_2$, $CH_2$C$H_3$), 0.21 (m, 1 H, C$H_2$) ppm. $^{13}$C-{$^1$H}NMR (101 MHz, $C_6D_6$, 25 °C): $\delta$ = 156.3, 142.7, 142.4, 138.0, 136.9 and 126.9 ($C_{ipso}$-Ar), 125.8, 125.2, 125.1 and 124.5 (*C*H-Ar), 66.2 (*C*H), 65.7 and 65.2 (Ar*C*$H_2$N), 59.4, 52.0 and 51.5 (*C*$H_2$), 36.1, 35.9, 34.9 and 34.8 [*C*($CH_3$)$_3$], 32.3, 32.2, 31.5, 31.0 [C(*C*$H_3$)$_3$], 27.1 and 22.5 (*C*$H_2$), 11.2 ($CH_2$*C*$H_3$) ppm. *Minor isomer*: $^1$H NMR (400 MHz, $C_6D_6$, 25 °C): $\delta$ = 7.52 (d, $^4J_{HH}$ = 2.1 Hz, 1 H, C*H*-Ar), 7.48 (d, $^4J_{HH}$ = 2.1 Hz, 1 H, C*H*-Ar), 7.12 (d, $^4J_{HH}$ = 1.9 Hz, 1 H, C*H*-Ar), 7.09 (d, $^4J_{HH}$ = 1.8 Hz, 1 H, C*H*-Ar), 5.68 (d, $^2J_{HH}$ = 14.2 Hz, 1 H, ArC$H_2$N), 5.42 (d, $^2J_{HH}$ = 13.1 Hz, 1 H, ArC$H_2$N), 3.33 (d, $^2J_{HH}$ = 14.2 Hz, 1 H, ArC$H_2$N), 3.25 (d, $^2J_{HH}$ = 13.2 Hz, 1 H, ArC$H_2$N), 1.74 [s, 9 H, C(C$H_3$)$_3$], 1.45 [s, 9 H, C(C$H_3$)$_3$], 1.44 [s, 9 H, C(C$H_3$)$_3$], 1.40 [s, 9 H, C(C$H_3$)$_3$] ppm. The other peaks are overlapped by the peaks of the major isomer. $^{13}$C-{$^1$H} NMR (101 MHz, $C_6D_6$, 25 °C): $\delta$ = 158.9, 157.6, 140.6, 140.5, 135.7 and 126.2 ($C_{ipso}$-Ar), 126.2, 125.4 and 125.1 (*C*H-Ar), 125.0 ($C_{ipso}$-Ar), 124.8 (*C*H-Ar), 66.6 (Ar*C*$H_2$N), 66.4 (*C*H), 66.2 (Ar*C*$H_2$N), 59.0, 51.4 and 49.2 (*C*$H_2$), 36.0, 35.8, 35.7 and 34.7 [*C*($CH_3$)$_3$], 32.4, 32.3, 31.9, 30.6 [C(*C*$H_3$)$_3$], 26.2 and 21.2 (*C*$H_2$), 11.9 ($CH_2$*C*$H_3$) ppm. $C_{37}H_{58}Cl_2N_2O_2Zr$·($C_4H_8O$) (796.64): calcd. C 57.02, H 7.69, N 3.74; found C 57.01, H 8.48, N 3.36.

**[ZrL$^1$(CH$_2$Ph)$_2$] (8):** A solution of **H$_2$L$^1$** (456 mg, 1 mmol) in toluene was slowly added to a solution of Zr($CH_2Ph$)$_4$ (539 mg, 1 mmol) in the same solvent. The solution was stirred at room temperature for 2 h. All the volatiles were removed under reduced pressure and the residue was washed with pentane to give a yellow solid; yield 670 mg, 83%. $^1$H NMR (500 MHz, $C_6D_6$, 25 °C): $\delta$ = 7.73 (d, $^3J_{HH}$ = 7.4 Hz, 2 H, $CH_2$*Ph*), 7.63 (d, $^4J_{HH}$ = 2.4 Hz, 1 H, C*H*-Ar), 7.58 (d, $^4J_{HH}$ = 2.4 Hz, 1 H, C*H*-Ar), 7.39 (t, $^3J_{HH}$ = 7.7 Hz, 2 H, $CH_2$*Ph*), 7.04 (t, $^3J_{HH}$ = 7.3 Hz, 1 H, $CH_2$*Ph*), 6.96 (d, $^4J_{HH}$ = 2.3 Hz, 1 H, C*H*-Ar), 6.90 (m, 3 H C*H*-Ar, $CH_2$*Ph*), 6.72 (t, $J_{HH}$ = 7.6 Hz, 2 H, $CH_2$*Ph*), 6.56 (t, $J_{HH}$ = 7.2 Hz, 1 H, $CH_2$*Ph*), 3.36 (d, $^2J_{HH}$ = 14.3 Hz, 1 H, ArC$H_2$N), 3.06 (d, $^2J_{HH}$ = 14.3 Hz, 1 H, ArC$H_2$N), 2.90 (d, $^2J_{HH}$ = 14.3 Hz, 1 H, ArC$H_2$N), 2.79 [m, 3 H, C$H_2$Ph, ArC$H_2$N, NC*H*($CH_3$)$CH_2$N], 2.67 (m, 2 H, C$H_2$Ph), 2.55 (d, $^2J_{HH}$ = 9.8 Hz, 1 H, C$H_2$Ph), 2.20 [t, $^2J_{HH}$ = 13.0 Hz, 1 H, NCH($CH_3$)C$H_2$N], 1.89 [s, 9 H, C(C$H_3$)$_3$], 1.88 [s, 9 H, C(C$H_3$)$_3$], 1.71 (s, 3 H, NC$H_3$), 1.39 (s, 3 H, NC$H_3$), 1.35 [s, 9 H, C(C$H_3$)$_3$], 1.34 [s, 9 H, C(C$H_3$)$_3$], 0.68 [dd, $^3J_{HH}$ = 3.0, $^2J_{HH}$ = 13.0 Hz, 1 H, NCH($CH_3$)C$H_2$N], 0.62 [d, $^3J_{HH}$ = 6.7 Hz, 3 H, NCH(C$H_3$)$CH_2$N] ppm. $^{13}$C-{$^1$H} NMR (126 MHz, $C_6D_6$, 25 °C): $\delta$ = 159.0 and 158.0 ($C_{ipso}$-Ar), 150.2 and 148.0 ($C_{ipso}$-Ph), 141.8, 141.4, 137.1 and 136.4 ($C_{ipso}$-Ar), 128.8, 128.1, 127.8 and 127.6 ($CH_2$*Ph*), 127.0 and 126.1 ($C_{ipso}$-Ar), 125.2, 125.1, 124.9 and 124.7 (*C*H-Ar), 122.6 and 120.6 ($CH_2$*Ph*), 68.6 (*C*$H_2$Ph), 66.6 [*C*$H_2$Ph, NCH($CH_3$)*C*$H_2$N], 61.0 and 57.2 (Ar*C*$H_2$N), 51.6 [N*C*H($CH_3$)-$CH_2$N], 49.7 and 46.7 [N(*C*$H_3$)$_2$], 36.1, 36.0, 34.8 and 34.7 [*C*($CH_3$)$_3$], 32.3, 31.3 and 31.0 [C(*C*$H_3$)$_3$], 8.2 [NCH(*C*$H_3$)$CH_2$N] ppm. $^{13}$C NMR (101 MHz, $C_6D_6$, 25 °C): $\delta$ = 68.6 (t, $^1J_{CH}$ = 123 Hz, Zr*C*$H_2$Ph), 66.6 (t, $^1J_{CH}$ = 121 Hz, Zr*C*$H_2$Ph) ppm. $C_{49}H_{70}N_2O_2Zr$ (809.77): calcd. C 72.63, H 8.71, N 3.46; found C 71.70, H 8.72, N 3.44; the low carbon content obtained results from the extreme instability of the complex; although the NMR spectra reveal the high purity of the compound (see Supporting Information), attempts to obtain good elemental analysis failed.

**[ZrL$^2$(CH$_2$Ph)$_2$] (9). Method A:** A solution of **H$_2$L$^2$** (220 mg, 0.48 mmol) in toluene was slowly added to a solution of Zr($CH_2Ph$)$_4$ (273 mg, 0.48 mmol) in the same solvent. After stirring for 2 h at room temperature the volatiles were removed under reduced pressure and the residue was washed with pentane to give a yellow solid; yield 404 mg, 70%.

**Method B:** A 1 M solution of $PhCH_2MgCl$ in $Et_2O$ (0.56 mL, 0.51 mmol) was slowly added to a solution of **7** in $Et_2O$ (185 mg,

  

0.26 mmol) and the mixture was stirred for 2 h. The yellow solution was filtered and the solvent removed under reduced pressure to give a yellow solid; yield 213 mg, 59%. $^1$H NMR (500 MHz, $C_6D_6$, 25 °C): $\delta$ = 7.59 (m, 4 H, C*H*-Ar, $CH_2$*Ph*), 7.37 (t, $^3J_{HH}$ = 7.7 Hz, 2 H, $CH_2$*Ph*), 7.02 (t, $^3J_{HH}$ = 7.1 Hz, 1 H, $CH_2$*Ph*), 6.94 (m, 3 H, C*H*-Ar, $CH_2$*Ph*), 6.86 (s, 1 H, C*H*-Ar), 6.76 (t, $^3J_{HH}$ = 7.6 Hz, 2 H, $CH_2$*Ph*), 6.59 (t, $^3J_{HH}$ = 6.9 Hz, 1 H, $CH_2$*Ph*), 3.64 (d, $^2J_{HH}$ = 13.4 Hz, 1 H, ArC$H_2$N), 2.93 (m, 2 H, ArC$H_2$N, C$H_2$Ph), 2.86 (m, 2 H, C$H_2$Ph, C$H_2$), 2.79 (m, 2 H, C$H_2$Ph), 2.73 (m, 2 H, ArC$H_2$N, *C*H), 2.58 (m, 2 H, ArC$H_2$N, C$H_2$), 2.37 (m, 2 H, C$H_2$), 2.24 (m, 1 H, C$H_2$), 1.91 [s, 9 H, C(C$H_3$)$_3$], 1.79 [s, 9 H, C(C$H_3$)$_3$], 1.35 [s, 9 H, C(C$H_3$)$_3$], 1.34 [s, 9 H, C(C$H_3$)$_3$], 1.29 (m, 1 H, C$H_2$), 0.88 (m, 2 H, C$H_2$), 0.68 (m, 1 H, C$H_2$), 0.36 (t, $^2J_{HH}$ = 10.9 Hz, 1 H, C$H_2$), 0.29 (t, $^3J_{HH}$ = 7.3 Hz, 3 H, $CH_2$C$H_3$) ppm. $^{13}$C–{$^1$H} NMR (126 MHz, $C_6D_6$, 25 °C): $\delta$ = 158.6 and 157.4 ($C_{ipso}$-Ar), 148.9 and 148.6 ($C_{ipso}$-Ph), 141.9, 141.5, 137.1 and 136.6 ($C_{ipso}$-Ar), 129.2, 128.7, 128.2 and 127.9 ($CH_2$*Ph*), 126.6 and 126.1 ($C_{ipso}$-Ar), 125.2, 124.7 and 124.3 (*C*H-Ar), 122.2 and 120.7 ($CH_2$*Ph*), 69.1 and 68.3 (*C*$H_2$Ph), 65.7 and 64.6 (Ar*C*$H_2$N), 64.2 (*C*H), 60.0, 52.2 and 51.9 (*C*$H_2$), 36.1, 36.0, 34.8 and 34.7 [*C*(CH$_3$)$_3$], 32.3, 32.2, 31.3, 31.1 [C(*C*H$_3$)$_3$], 28.7 and 23.6 (*C*$H_2$), 11.7 ($CH_2$*C*$H_3$) ppm. $^{13}$C NMR (101 MHz, $C_6D_6$, 25 °C): $\delta$ = 69.1 (t, $^1J_{CH}$ = 124 Hz, Zr*C*$H_2$Ph), 68.3 (t, $^1J_{CH}$ = 112 Hz, Zr*C*$H_2$Ph) ppm. EA calculated for $C_{51}H_{72}N_2O_2Zr$ (835.78): C 73.24, H 8.68, N 3.35; found C 71.34, H 8.65, N 3.34; the low carbon content obtained results from the extreme instability of the complex; although the NMR spectra reveal the high purity of the compound (see Supporting Information), attempts to obtain good elemental analysis failed.

**[TiL$^1$(CH$_2$Ph)][PhCH$_2$B(C$_6$F$_5$)$_3$] (10):** In a NMR tube, **5** (7.00 mg, 9.13 μmol) was treated with one equivalent of B($C_6F_5$)$_3$ (4.67 mg, 9.13 μmol) in $C_6D_5Br$ (0.6 mL). After 10 min, the NMR spectrum of the dark orange solution revealed the quantitative formation of **10**. $^1$H NMR (500 MHz, $C_6D_5Br$, 25 °C): $\delta$ = 7.44 (s, 1 H, C*H*-Ar), 7.39 (s, 1 H, C*H*-Ar), 7.27 (m, 4 H, $CH_2$*Ph*), 7.23 (s, 1 H, C*H*-Ar), 7.10 (m, 2 H, $CH_2$*Ph*), 7.06 (m, 1 H, $CH_2$*Ph*), 6.92 (m, 2 H, $CH_2$*Ph*), 6.83 (s, 1 H, C*H*-Ar), 6.78 (t, $^3J_{HH}$ = 6.5 Hz, 1 H, $CH_2$*Ph*), 3.77 (d, $^2J_{HH}$ = 14.1 Hz, 1 H, ArC$H_2$N), 3.70 (m, 2 H, ArC$H_2$N), 3.36 (d, $^2J_{HH}$ = 13.9 Hz, 1 H, ArC$H_2$N), 3.29 (s, 2 H, BC$H_2$Ph), 3.25 (s, 2 H, TiC$H_2$Ph), 2.90 [m, 2 H, NC*H*(CH$_3$)CH$_2$N, NCH(CH$_3$)C$H_2$N], 2.22 [s, 3 H, N(C$H_3$)$_2$], 2.19 [s, 3 H, N(C$H_3$)$_2$], 2.09 [m, 1 H, NCH(CH$_3$)C$H_2$N], 1.46, 1.37, 1.32 and 1.20 [s, 9 H, C(C$H_3$)$_3$], 0.74 [d, $^3J_{HH}$ = 4.4 Hz, 3 H, NCH(C$H_3$)CH$_2$N] ppm. $^{13}$C-{$^1$H} NMR (126 MHz, $C_6D_5Br$, 25 °C): $\delta$ = 161.7 and 159.7 ($C_{ipso}$-Ar), 149.4 [br., B($C_6F_5$)$_3$], 148.6 ($C_{ipso}$-*Ph*CH$_2$B), 147.6 [br., B($C_6F_5$)$_3$], 147.4 ($C_{ipso}$-*Ph*CH$_2$Ti), 147.4 and 145.2 ($C_{ipso}$-Ar), 138.5, 137.4, 136.5 and 135.5 [br., B($C_6F_5$)$_3$], 135.1 and 134.8 ($C_{ipso}$-Ar), 131.2, 129.6, 128.8, 128.4, 128.2, 127.8, 127.0, 126.4 and 125.8 ($CH_2$*Ph*), 125.1, 124.9 and 124.8 (*C*H-Ar), 123.8 and 123.6 ($C_{ipso}$-Ar), 122.7 ($CH_2$*Ph*), 104.0 (Ar*C*H$_2$N), 68.6 [NCH(CH$_3$)*C*H$_2$N], 55.6 (Ti*C*H$_2$Ph), 52.4 [N*C*H(CH$_3$)CH$_2$N], 50.2 [N(*C*H$_3$)$_2$], 49.8 (ArCH$_2$N), 47.9 [N(*C*H$_3$)$_2$], 34.9, 34.7, 34.5 and 34.3 [*C*(CH$_3$)$_3$], 31.4 (B*C*H$_2$Ph), 31.2, 31.1, 29.9 and 29.8 [C(*C*H$_3$)$_3$], 7.0 [NCH(*C*H$_3$)CH$_2$N] ppm. $^{19}$F NMR (376 MHz, $C_6D_5Br$, 25 °C): $\delta$ = –130.59 (br., 6 F, *o*-$C_6F_5$), –163.66 (br., 3 F, *p*-$C_6F_5$), –166.46 (br., 6 F, *m*-$C_6F_5$) ppm. [|$\Delta\delta$(*m*,*p*-F)|] = 2.80.

**[ZrL$^1$(CH$_2$Ph)][PhCH$_2$B(C$_6$F$_5$)$_3$] (11):** In a NMR tube, **8** (8.00 mg, 9.87 μmol) was treated with one equivalent of B($C_6F_5$)$_3$ (5.00 mg, 9.87 μmol) in $C_6D_5Br$ (0.6 mL). After 10 min, the NMR spectrum of the light yellow solution revealed the quantitative formation of **11**. $^1$H NMR (500 MHz, $C_6D_5Br$, 25 °C): $\delta$ 7.50 (m, 4 H, C*H*-Ar, $CH_2$*Ph*), 7.19 (t, 2 H, $^3J_{HH}$ = 7.5 Hz, $CH_2$*Ph*), 7.11 (m, 3 H, $CH_2$*Ph*), 7.07 (d, 1 H, $^4J_{HH}$ = 1.9 Hz, C*H*-Ar), 6.99 (d, 1 H, $^4J_{HH}$ = 2.1 Hz, C*H*-Ar), 6.92 (t, 2 H, $^3J_{HH}$ = 7.6 Hz, $CH_2$*Ph*), 6.77 (t, 1 H, $^3J_{HH}$ = 7.3 Hz, $CH_2$*Ph*), 3.61 (d, 1 H, $^2J_{HH}$ = 14.3 Hz, ArC$H_2$N), 3.51 (d, 1 H, $^2J_{HH}$ = 14.4 Hz, ArC$H_2$N), 3.39 (d, 1 H, $^2J_{HH}$ = 14.5 Hz, ArC$H_2$N), 3.31 (s, 2 H, BC$H_2$Ph), 3.28 (d, 1 H, $^2J_{HH}$ = 14.5 Hz, ArC$H_2$N), 2.98 [m, 1 H, NC*H*(CH$_3$)CH$_2$N], 2.94 (s, 2 H, ZrC$H_2$Ph), 2.47 [m, 1 H, NCH(CH$_3$)C$H_2$N], 2.04 [s, 3 H, N(C$H_3$)$_2$], 1.77 [s, 3 H, N(C$H_3$)$_2$], 1.52 [s, 18 H, C(C$H_3$)$_3$], 1.33 [m, 1 H, NCH(CH$_3$)C$H_2$], 1.32 [s, 9 H, C(C$H_3$)$_3$], 1.30 [s, 9 H, C(C$H_3$)$_3$], 0.92 [d, 3 H, $^3J_{HH}$ = 6.6 Hz, NCH(C$H_3$)CH$_2$N] ppm. $^{13}$C–{$^1$H} NMR (126 MHz, $C_6D_5Br$, 25 °C): $\delta$ 155.5 and 154.8 ($C_{ipso}$-Ar), 149.5 [br., B($C_6F_5$)$_3$], 148.8 ($C_{ipso}$-*Ph*CH$_2$B), 147.6 [br., B($C_6F_5$)$_3$], 144.8 and 144.7 ($C_{ipso}$-Ar), 138.5, 137.5 and 136.5 [br., B($C_6F_5$)$_3$], 135.8 ($C_{ipso}$-Ar), 135.5 [br., B($C_6F_5$)$_3$], 135.2 ($C_{ipso}$-Ar), 134.3 and 131.8 ($CH_2$*Ph*), 131.6 ($C_{ipso}$-*Ph*CH$_2$Zr), 131.2, 129.6, 128.9, 127.0 and 126.4 ($CH_2$*Ph*), 125.6 and 125.5 (*C*H-Ar), 125.2 ($C_{ipso}$-Ar), 125.2 and 125.0 (*C*H-Ar), 124.3 ($C_{ipso}$-Ar), 122.6, 122.5 and 121.9 ($CH_2$*Ph*), 72.6 (Zr*C*H$_2$Ph), 67.5 [NCH(CH$_3$)*C*H$_2$N], 60.9 (Ar*C*H$_2$N), 57.0 (Ar*C*H$_2$N), 52.3 [N*C*H(CH$_3$)CH$_2$N], 52.0 and 47.4 [N(*C*H$_3$)$_2$], 35.0, 34.9 and 34.2 [*C*(CH$_3$)$_3$], 31.45 (B*C*H$_2$Ph), 31.33, 31.29 and 30.0 [C(*C*H$_3$)$_3$], 7.4 [NCH(*C*H$_3$)CH$_2$N] ppm. $^{13}$C NMR (126 MHz, $C_6D_5Br$, 25 °C): $\delta$ 72.6 (t, $^1J_{CH}$ = 139 Hz, Zr*C*H$_2$Ph) ppm. $^{19}$F NMR (376 MHz, $C_6D_5Br$, 25 °C): $\delta$ –130.16 (d, 6 F, $^3J_{FF}$ = 22.6 Hz, *o*-$C_6F_5$), –163.59 (t, 3 F, $^3J_{FF}$ = 22.6 Hz, *p*-$C_6F_5$), –166.30 (t, 6 F, $^3J_{FF}$ = 22.6 Hz, *m*-$C_6F_5$) ppm. [|$\Delta\delta$(*m*,*p*-F)|] = 2.71.

**[ZrL$^2$(CH$_2$Ph)][PhCH$_2$B(C$_6$F$_5$)$_3$] (12):** In a NMR tube, **9** (7.00 mg, 8.37 μmol) was treated with one equivalent of B($C_6F_5$)$_3$ (4.28 mg, 8.37 μmol) in $C_6D_5Br$ (0.6 mL). After 10 min, the NMR spectrum of the light yellow solution revealed the quantitative formation of **12**. $^1$H NMR (500 MHz, $C_6D_5Br$, 25 °C): $\delta$ = 7.43 (m, 5 H, C*H*-Ar, $CH_2$*Ph*), 7.37 (s, 1 H, C*H*-Ar), 7.25 (s, 1 H, C*H*-Ar), 7.13 (d, $^3J_{HH}$ = 7.2 Hz, 3 H, $CH_2$*Ph*), 6.96 (m, 2 H, $CH_2$*Ph*), 6.85 (s, 1 H, C*H*-Ar), 6.81 (t, $^3J_{HH}$ = 7.1 Hz, 1 H, $CH_2$*Ph*), 4.42 (d, $^2J_{HH}$ = 13.4 Hz, 1 H, ArC$H_2$N), 3.62 (m, 1 H, *C*H), 3.52 (d, $^2J_{HH}$ = 14.8 Hz, 1 H, ArC$H_2$N), 3.33 (s, 2 H, BC$H_2$Ph), 3.17 (d, $^2J_{HH}$ = 14.9 Hz, 1 H, ArC$H_2$N), 3.10 (d, $^2J_{HH}$ = 13.5 Hz, 1 H, ArC$H_2$N), 2.97 (m, 1 H, C$H_2$), 2.73 (t, $^3J_{HH}$ = 9.1 Hz, 1 H, C$H_2$), 2.55 (s, 2 H, ZrC$H_2$Ph), 2.49 (t, $^2J_{HH}$ = 13.5 Hz, 1 H, C$H_2$), 2.40 (m, 2 H, $CH_2$C$H_3$), 2.02 (d, $^2J_{HH}$ = 13.4 Hz, 1 H, C$H_2$), 1.69 (m, 1 H, C$H_2$), 1.47 (m, 1 H, C$H_2$), 1.34 [s, 9 H, C(C$H_3$)$_3$], 1.27 [s, 9 H, C(C$H_3$)$_3$], 1.23 [s, 9 H, C(C$H_3$)$_3$], 120 [s, 9 H, C(C$H_3$)$_3$], 1.20 (1 H, C$H_2$), 0.97 (t, $^3J_{HH}$ = 6.8 Hz, 1 H, $CH_2$C$H_3$), 0.90 (m, 1 H, C$H_2$) ppm. $^{13}$C-{$^1$H} NMR (126 MHz, $C_6D_5Br$, 25 °C): $\delta$ = 157.7 and 155.3 ($C_{ipso}$-Ar), 149.4 [br., B($C_6F_5$)$_3$], 148.6 ($C_{ipso}$-*Ph*CH$_2$B), 147.5 [br., B($C_6F_5$)$_3$], 145.5 and 145.4 ($C_{ipso}$-Ar), 138.5 and 137.5 [br., B($C_6F_5$)$_3$], 136.8 ($C_{ipso}$-Ar), and 136.5 [br., B($C_6F_5$)$_3$], 136.1 ($C_{ipso}$-Ar), 135.8 ($C_{ipso}$-*Ph*CH$_2$Zr), 135.5 [br., B($C_6F_5$)$_3$], 132.9, 131.2, 129.6, 128.8, 128.4, 127.1 and 126.4 ($CH_2$*Ph*), 125.4 and 125.2 (*C*H-Ar), 122.8 and 122.4 ($CH_2$*Ph*), 122.0 ($C_{ipso}$-Ar), 121.9 (*C*H-Ar), 121.6 ($C_{ipso}$-Ar), 68.8 (Zr*C*H$_2$Ph), 64.4 (*C*H), 59.2 and 58.3 (Ar*C*H$_2$N), 56.6 and 55.5 (*C*H$_2$), 52.9 (*C*H$_2$CH$_3$), 34.8, 34.5, 34.3 and 34.1 [*C*(CH$_3$)$_3$], 31.4 (B*C*H$_2$Ph), 31.3, 31.2, 30.2 and 29.7 [C(*C*H$_3$)$_3$], 24.3 and 21.5 (*C*H$_2$), 14.6 (CH$_2$*C*H$_3$) ppm. $^{19}$F NMR (376 MHz, $C_6D_5Br$, 25 °C): $\delta$ = –130.68 (d, $^3J_{FF}$ = 22.6 Hz, 6 F, *o*-$C_6F_5$), –163.60 (t, $^3J_{FF}$ = 18.8 Hz, 3 F, *p*-$C_6F_5$), –166.44 (t, $^3J_{FF}$ = 22.6 Hz, 6 F, *m*-$C_6F_5$) ppm. [|$\Delta\delta$(*m*,*p*-F)|] = 2.84.

**[ZrL$^1$(CH$_2$Ph)][B(C$_6$F$_5$)$_4$] (13):** In a NMR tube, **8** (7.00 mg, 8.64 μmol) was treated with one equivalent of [PhNMe$_2$H][B($C_6F_5$)$_4$] (6.92 mg, 8.64 μmol) in $C_6D_5Br$ (0.6 mL). After 10 min, the NMR spectrum of the light yellow solution revealed the quantitative formation of **13**, toluene and free PhNMe$_2$. $^1$H NMR (500 MHz, $C_6D_5Br$, 25 °C): $\delta$ = 7.54 (m, 4 H, C*H*-Ar, $CH_2$*Ph*), 7.18 [m, 6 H, N*Ph*(CH$_3$)$_2$, $CH_3$*Ph*, $CH_2$*Ph*], 7.07 (m, 5 H, C*H*-Ar, $CH_2$*Ph*, $CH_3$*Ph*), 6.98 (s, 1 H, C*H*-Ar), 6.80 [t, 1 H, $^3J_{HH}$ = 7.1 Hz, N*Ph*(CH$_3$)$_2$], 6.60 [m, 2 H, N*Ph*(CH$_3$)$_2$], 3.55 (d, 1 H, $^2J_{HH}$ =

  

14.3 Hz, ArC$H_2$N), 3.46 (d, 1 H, $^2J_{HH}$ = 14.4 Hz, ArC$H_2$N), 3.33 (d, 1 H, $^2J_{HH}$ = 14.2 Hz, ArC$H_2$N), 3.21 (d, 1 H, $^2J_{HH}$ = 14.3 Hz, ArC$H_2$N), 2.94 [m, 3 H, NC$H$(CH$_3$)CH$_2$N, ZrC$H_2$Ph], 2.56 [s, 6 H, NPh(C$H_3$)$_2$], 2.45 [t, 1 H, $^2J_{HH}$ = 13.3 Hz, NCH(CH$_3$)C$H_2$N], 2.18 (s, 3 H, C$H_3$Ph), 2.00 [s, 3 H, N(C$H_3$)$_2$], 1.72 [s, 3 H, N(C$H_3$)$_2$], 1.54 [s, 9 H, C(C$H_3$)$_3$], 1.53 [s, 9 H, C(C$H_3$)$_3$], 1.34 [s, 9 H, C(C$H_3$)$_3$], 1.33 [s, 9 H, C(C$H_3$)$_3$], 1.26 [m, 1 H, NCH(CH$_3$)-C$H_2$N], 0.88 [d, 3 H, $^3J_{HH}$ = 6.4 Hz, NCH(C$H_3$)CH$_2$N] ppm. $^{13}$C-{$^1$H} NMR (126 MHz, $C_6D_5Br$, 25 °C): $\delta$ = 155.6 and 154.9 ($C_{ipso}$-Ar), 149.5 and 147.5 [br., B($C_6F_5$)$_3$], 144.9 and 144.8 ($C_{ipso}$-Ar), 139.3 [br., B($C_6F_5$)$_3$], 137.4 [br., B($C_6F_5$)$_3$], 135.9 ($C_{ipso}$-Ar), 135.5 [br., B($C_6F_5$)$_3$], 135.2 ($C_{ipso}$-Ar), 134.2 and 131.8 (*Ph*), 131.5 ($C_{ipso}$-*Ph*CH$_2$Zr), 131.2, 129.6, 129.2, 128.9, 128.1 and 127.9 (*Ph*), 126.4, 125.5 and 125.3 (*C*H-Ar), 125.2 ($C_{ipso}$-Ar), 124.9 (*C*H-Ar), 124.2 ($C_{ipso}$-Ar), 122.4, 121.9, 118.5 and 113.3 (*Ph*), 72.5 (Zr*C*H$_2$Ph), 67.4 [NCH(CH$_3$)*C*H$_2$N], 60.8 and 56.8 (Ar*C*H$_2$N), 52.2 [N*C*H(CH$_3$)-CH$_2$N], 51.9 and 47.3 [N(*C*H$_3$)$_2$], 41.0 [NPh(*C*H$_3$)$_2$], 35.0, 34.9 and 34.2 [*C*(CH$_3$)$_3$], 31.23, 31.18 and 30.0 [C(*C*H$_3$)$_3$], 21.2 (*C*H$_3$Ph), 7.1 [NCH(*C*H$_3$)CH$_2$N] ppm. $^{19}$F NMR (470 MHz, $C_6D_5Br$, 25 °C): $\delta$ = –132.14 (br., 8 F, *o*-C$_6F_5$), –162.54 (t, 4 F, $^3J_{FF}$ = 23.5 Hz, *p*-C$_6F_5$), –166.38 (t, 8 F, $^3J_{FF}$ = 18.8 Hz, *m*-C$_6F_5$) ppm.

**General Procedure for Small-Scale Ethylene and Propylene Polymerization:** In the glovebox, precatalyst stock solutions were prepared (0.01 M) in toluene (2 mL, **6** and **7**) or bromobenzene (2 mL, **5**, **8** and **9**) and stored at –37 °C. B($C_6F_5$)$_3$, [PhNMe$_2$H][B($C_6F_5$)$_4$] (0.01 M in bromobenzene) and TIBAO (0.1 M in toluene) stock solutions were also prepared and stored. In the polymerization runs with **6** and **7**, a 100 mL Büchi glass autoclave containing one Teflon®-coated stirrer bar was charged with dry toluene (9 mL), precatalyst solution (0.5 mL) and MMAO (0.533 mL, 7 % Al in heptanes) and then pressurized with 5 bar of the monomer. In the polymerization runs with **5**, **8** and **9**, a 100 mL Büchi glass autoclave with a Teflon® coated stirrer bar was charged with dry toluene (9 mL), precatalyst solution (0.5 mL) and B($C_6F_5$)$_3$ or [PhNMe$_2$H][B($C_6F_5$)$_4$] solution (0.5 mL) and then pressurized with the monomer to a pressure of 5 bar. When TIBAO was added as a scavenger the autoclaves were charged with toluene (8 mL), precatalyst solution (0.5 mL), TIBAO solution (1 mL) and B($C_6F_5$)$_3$ or [PhNMe$_2$H][B($C_6F_5$)$_4$] solution (0.5 mL) and then pressurized with the monomer to a pressure of 5 bar. The mixture in the reactor was stirred for 30 min with continuous supply of monomer. The polymerization was ended by venting the reactor and subsequent addition of acidified methanol (5% HCl).

**Polyethylene:** The polymeric material was collected and washed several times with ethanol and dried in a vacuum oven at 80 °C overnight. The polymer was analyzed by HT-GPC.

**Polypropylene:** The polymeric material was poured into ca. 100 mL of stirring ethanol and the solvents were removed under reduced pressure. The polymer was analyzed by HT-GPC and $^{13}$C-{$^1$H} NMR spectroscopy. Typical NMR analysis of the samples showed that the polypropylene obtained is atactic.

**General Procedure for 1-Hexene Polymerization:** A solution of precatalyst (0.5 mL, 0.01 M in bromobenzene) was dissolved in 1-hexene (9 mL) at room temperature under nitrogen and then a solution of B($C_6F_5$)$_3$ (0.5 mL, 0.01 M in bromobenzene) was added. The reaction mixture was stirred for 30 min. The solvent and remaining monomer were removed under reduced pressure to yield poly(1-hexene) as a colourless sticky oil. The polymer was analyzed by HT-GPC and $^{13}$C-{$^1$H} NMR spectroscopy. $^{13}$C-{$^1$H} NMR (500 MHz, $CD_2Cl_2CD_2Cl_2$, ppm): $\delta$ = 40.4 (br., *C*H$_2$), 34.3 (br., *C*H$_2$), 32.4 (*C*H), 28.7 (*C*H$_2$), 28.4 (*C*H$_2$), 23.5 (*C*H$_2$), 14.5 (*C*H$_3$) ppm.

**General Procedures for X-ray Crystallography:** Colourless crystals of **H$_2$L$^1$** and **H$_2$L$^2$** were obtained from methanol solutions at room temperature. Crystals of **3** (orange), **6** (colourless) and **8** (yellow) were grown from toluene solutions –37 °C. Crystallographic data were collected at *Instituto Superior Técnico* and at the *University of Groningen*. Crystals of air/moisture sensitive compounds were selected inside the glovebox, covered with polyfluoroether oil and mounted on a nylon loop. The data were collected using graphite monochromated Mo-$K_\alpha$ radiation ($\lambda$ = 0.71073 Å) with Bruker AXS-KAPPA APEX II and Bruker SMART APEX CCD diffractometers equipped with an Oxford Cryosystem open-flow nitrogen cryostat. Cell parameters were retrieved using Bruker SMART software and refined using Bruker SAINT on all observed

Table 4. Selected crystallographic experimental data and structure refinement parameters for **H$_2$L$^1$**, **H$_2$L$^2$**, **3**, **6** and **8**.

| | **H$_2$L$^1$** | **H$_2$L$^2$** | **3** | **6** | **8** |
|---|---|---|---|---|---|
| Empirical formula | $C_{35}H_{58}N_2O_2$ | $C_{37}H_{60}N_2O_2$ | $C_{40}H_{65}ClN_2O_3Ti\cdot(C_7H_8)$ | $C_{35}H_{56}Cl_2N_2O_2Zr$ | $C_{49}H_{10}N_2O_2Zr\cdot(C_7H_8)$ |
| Formula weight | 538.83 | 564.87 | 797.43 | 697.93 | 902.47 |
| Temperature [K] | 150(2) | 150(2) | 100(1) | 150(2) | 100(1) |
| Crystal system | orthorhombic | monoclinic | triclinic | monoclinic | monoclinic |
| Space group | *Pbca* | $P2_1$ | $P\bar{1}$ | $P2_1/c$ | $P2_1/c$ |
| *a* [Å] | 29.284(4) | 15.2340(15) | 9.669(3) | 15.7740(11) | 10.5347(15) |
| *b* [Å] | 14.6150(17) | 29.903(3) | 11.044(4) | 16.1970(11) | 24.979(4) |
| *c* [Å] | 31.861(4) | 15.4060(18) | 11.694(4) | 18.4740(13) | 18.993(3) |
| $\alpha$ [°] | 90 | 90 | 99.800(5) | 90 | 90 |
| $\beta$ [°] | 90 | 95.267(6) | 109.598(4) | 99.864(3) | 90.602(2) |
| $\gamma$ [°] | 90 | 90 | 93.657(4) | 90 | 90 |
| *V* [Å$^3$] | 13636(3) | 6988.5(13) | 1149.4(7) | 4650.2(6) | 4997.7(13) |
| *Z*, $\rho_{calc}$ [g cm$^{-3}$] | 16, 1.050 | 8, 1.074 | 1, 1.152 | 4, 0.997 | 4, 1.199 |
| $\mu$ [mm$^{-1}$] | 0.064 | 0.065 | 0.284 | 0.376 | 0.261 |
| Crystal size | 0.40 × 0.30 × 0.20 | 0.30 × 0.25 × 0.25 | 0.38 × 0.32 × 0.23 | 0.40 × 0.20 × 0.05 | 0.53 × 0.44 × 0.35 |
| Crystal colour | colourless | colourless | orange | colourless | yellow |
| Crystal shape | block | block | block | plate | block |
| Reflections collected | 131094 | 97609 | 7448 | 68995 | 40092 |
| Unique refl. [*R*(int)] | 12088 [0.1741] | 23828 [0.0783] | 5928 [0.0390] | 8138 [0.0743] | 10518 [0.0390] |
| $R_1$ [$I > 2\sigma(I)$] | 0.0567 | 0.0577 | 0.1014 | 0.1073 | 0.0422 |
| $wR_2$ [$I > 2\sigma(I)$] | 0.1142 | 0.1247 | 0.3063 | 0.2484 | 0.0996 |
| GooF | 0.941 | 0.999 | 1.802 | 1.317 | 1.048 |
| Flack's parameter | | 0.6(9) | 0.04(8) | | |

  

reflections. Absorption corrections were applied using SADABS.[22] The structures were solved and refined using direct methods with programs SIR97,[23] SIR2004[24] or SHELXS-97.[25] All programs are included in the package of programs WINGX-Version 1.80.01[26] SHELXL.[27] Unless stated otherwise, all non-hydrogen atoms were refined anisotropically and the hydrogen atoms were inserted in idealized positions and allowed to refine riding on the parent carbon atom. Molecular diagrams were drawn with ORTEP-3 for Windows[28] or Mercury 1.4.2,[29] included in the software package. Compound **3** crystallizes in a noncentrosymmetric space group and the refinement of the Flack[30] parameter *x* resulted in a value of 0.04(8). $\mathbf{H_2L^2}$ cristallizes in a noncentrosymmetric space group but the absolute configuration could not be confirmed as the Friedel pairs were not measured, furthermore as there were no heavy atoms in the molecule, no significant anomalous dispersion could be obtained using Mo radiation. The poor quality of the crystals of **3** and **6** led to low quality data. The structures are included, as they are good enough to confirm the connectivity. Crystallographic data for $\mathbf{H_2L^1}$, $\mathbf{H_2L^2}$, **3**, **6** and **8** are presented in Table 4.

CCDC-823660 (for $\mathbf{H_2L^1}$), -823661 (for $\mathbf{H_2L^2}$), -823662 (for **6**), -821180 (for **8**) and -821181 (for **3**) contain the supplementary crystallographic data for this paper. These data can be obtained free of charge from The Cambridge Crystallographic Data Centre via www.ccdc.cam.uk/data_request/cif.

**Supporting Information** (see footnote on the first page of this article): Additional information for the molecular structures of $\mathbf{H_2L^1}$ and $\mathbf{H_2L^2}$; $^1$H NMR spectra of **8** and **9**.

## Acknowledgments

We thank Dr. Winfried P. Kretschmer (University of Bayreuth) for the HT-GPC analyses of the polymers. We thank the Portuguese NMR Network (IST-UTL Center) for providing access to the NMR facilities and the Fundação para a Ciência e Tecnologia (FCT) for financial support (PTDC/QUI/66187/2006 and fellowships SFRH/BD/28762/2006 and SFRH/BD/40279/2007).

[1] a) G. W. Coates, P. D. Hustad, S. Reinartz, *Angew. Chem.* **2002**, *114*, 2340; *Angew. Chem. Int. Ed.* **2002**, *41*, 2236–2257; b) V. C. Gibson, S. K. Spitzmesser, *Chem. Rev.* **2003**, *103*, 283–315; c) G. J. Domski, J. M. Rose, G. W. Coates, A. D. Bolig, M. Brookhart, *Prog. Polym. Sci.* **2007**, *32*, 30–92.

[2] a) J. D. Scollard, D. H. McConville, *J. Am. Chem. Soc.* **1996**, *118*, 10008–10009; b) R. Baumann, W. M. Davis, R. R. Schrock, *J. Am. Chem. Soc.* **1997**, *119*, 3830–3831.

[3] a) E. Y. Tshuva, I. Goldberg, M. Kol, Z. Goldschmidt, *Inorg. Chem. Commun.* **2000**, *3*, 611–614; b) E. Y. Tshuva, I. Goldberg, M. Kol, H. Weitman, Z. Goldschmidt, *Chem. Commun.* **2000**, 379–380; c) E. T. Tshuva, I. Goldberg, M. Kol, Z. Goldschmidt, *Organometallics* **2001**, *20*, 3017–3028; d) E. Y. Tshuva, I. Goldberg, M. Kol, Z. Goldschmidt, *Chem. Commun.* **2001**, 2120–2121; e) E. T. Tshuva, S. Groysman, I. Goldberg, M. Kol, Z. Goldschmidt, *Organometallics* **2002**, *21*, 662–670; f) S. Groysman, I. Goldberg, M. Kol, E. Genizi, Z. Goldschmidt, *Inorg. Chim. Acta* **2003**, *345*, 137–144; g) S. Groysman, I. Goldberg, M. Kol, *Organometallics* **2003**, *22*, 3013–3015; h) S. Groysman, E. Y. Tshuva, I. Goldberg, M. Kol, Z. Goldschmidt, M. Shuster, *Organometallics* **2004**, *23*, 5291–5299.

[4] S. Gendler, S. Groysman, Z. Goldschmidt, M. Shuster, M. Kol, *J. Polym. Sci. Polym. Chem. Ed.* **2006**, *44*, 1136–1146.

[5] S. Groysman, E. Y. Tshuva, D. Reshef, S. Gendler, I. Goldberg, M. Kol, Z. Goldschmidt, M. Shuster, G. Lidor, *Isr. J. Chem.* **2002**, *42*, 373–381.

[6] S. E. Reybuck, A. L. Lincoln, S. Ma, R. M. Waymouth, *Macromolecules* **2005**, *38*, 2552–2558.

[7] a) A. Yeori, I. Goldberg, M. Kol, *Macromolecules* **2007**, *40*, 8521–8523; b) S. Segal, A. Yeori, M. Shuster, Y. Rosenberg, M. Kol, *Macromolecules* **2008**, *41*, 1612–1617; c) A. Cohen, J. Kopilov, I. Goldberg, M. Kol, *Organometallics* **2009**, *28*, 1391–1405; d) E. Sergeeva, J. Kopilov, I. Goldberg, M. Kol, *Inorg. Chem.* **2009**, *48*, 8075–8077.

[8] R. D. R. S. Manian, R. Leino, O. Wichmann, A. Lehtonen, *Inorg. Chem. Commun.* **2009**, *12*, 1004–1006.

[9] a) S. Barroso, J. Cui, J. M. Carretas, A. Cruz, I. C. Santos, M. T. Duarte, J. P. Telo, N. Marques, A. M. Martins, *Organometallics* **2009**, *28*, 3449–3458; b) S. Barroso, P. Adão, F. Madeira, M. T. Duarte, J. C. Pessoa, A. M. Martins, *Inorg. Chem.* **2010**, *49*, 7452–7463.

[10] S. Barroso, A. M. Abreu, A. C. Araújo, A. M. Coelho, N. Maulide, A. M. Martins, *Synlett* **2010**, *16*, 2425–2428.

[11] E. Y. Tshuva, M. Versano, I. Goldberg, M. Kol, H. Weitman, Z. Goldschmidt, *Inorg. Chem. Commun.* **1999**, *2*, 371–373.

[12] a) N. Berova, L. Di Bari, G. Pescitelli, *Chem. Soc. Rev.* **2007**, *36*, 914–931; b) P. Adão, F. Avecilla, M. Bonchio, M. Carraro, J. C. Pessoa, I. Correia, *Eur. J. Inorg. Chem.* **2010**, 5568–5578.

[13] A. L. Rheingold, N. P. Robinson, J. Whelan, B. Bosnich, *Organometallics* **1992**, *11*, 1869–1876.

[14] a) L. G. Alves, M. A. Antunes, I. Matos, R. F. Munha, M. T. Duarte, A. C. Fernandes, M. M. Marques, A. M. Martins, *Inorg. Chim. Acta* **2010**, *363*, 1823–1830; b) T. Toupance, S. R. Dubberley, N. H. Rees, B. R. Tyrrell, P. Mountford, *Organometallics* **2002**, *21*, 1367–1382.

[15] a) A. D. Horton, J. de With, A. J. van der Linden, H. van de Weg, *Organometallics* **1996**, *15*, 2672–2674; b) A. D. Horton, J. de With, *Chem. Commun.* **1996**, 1375–1376; c) A. D. Horton, J. de With, *Organometallics* **1997**, *16*, 5424–5436.

[16] U. Zucchini, E. Albizzati, U. Giannini, *J. Organomet. Chem.* **1971**, *26*, 357–372.

[17] a) R. F. Jordan, R. E. LaPointe, N. C. Baenziger, G. D. Hinch, *Organometallics* **1990**, *9*, 1539–1545; b) M. Bochmann, S. J. Lancaster, *Organometallics* **1993**, *12*, 633–640; c) M. Bouwkamp, D. van Leusen, A. Meetsma, B. Hessen, *Organometallics* **1998**, *17*, 3645–3647; d) P.-J. Sinnema, K. Liekelema, O. K. B. Staal, B. Hessen, J. H. Teuben, *J. Mol. Catal. A* **1998**, *128*, 143–153.

[18] In accordance with Gibson's scale: G. J. P. Britovsek, V. C. Gibson, D. F. Wass, *Angew. Chem.* **1999**, *111*, 448; *Angew. Chem. Int. Ed.* **1999**, *38*, 428–447.

[19] a) P. T. Witte, A. Meetsma, B. Hessen, *J. Am. Chem. Soc.* **1997**, *119*, 10561–10562; b) B. F. Straub, F. Eisenträger, P. Hofmann, *Chem. Commun.* **1999**, 2507–2508.

[20] a) E. Tshuva, I. Goldberg, M. Kol, *Inorg. Chem.* **2001**, *40*, 4263–4270; b) A. J. Nielson, J. M. Waters, *Polyhedron* **2010**, *29*, 1715–1726; c) M. Mazzanti, J. M. Rosset, C. Floriani, A. Chiesi-Villa, C. Guastini, *J. Chem. Soc., Dalton Trans.* **1989**, 953–957.

[21] a) R. F. Jordan, R. E. LaPointe, P. K. Bradley, N. Baenziger, *Organometallics* **1989**, *8*, 2892–2903; b) A. G. Massey, A. Park, *J. Organomet. Chem.* **1964**, *2*, 245–250; c) H. Brand, J. A. Capriotti, J. Arnold, *Organometallics* **1994**, *13*, 4469–4473; d) R. R. Schrock, *J. Organomet. Chem.* **1976**, *122*, 209–225.

[22] G. M. Sheldrick, *SADABS, Program for Empirical Absorption Correction*, University of Göttingen, Germany, **1996**.

[23] A. Altomare, M. C. Burla, M. Camalli, G. L. Cascarano, C. Giacovazzo, A. Guagliardi, A. G. G. Moliterni, G. Polidori, R. Spagna, *J. Appl. Crystallogr.* **1999**, *32*, 115–119.

[24] M. C. Burla, R. Caliandro, M. Camalli, B. Carrozzini, G. L. Cascarano, L. De Caro, C. Giacovazzo, G. Polidori, R. Spagna, *J. Appl. Crystallogr.* **2005**, *38*, 381–388.

[25] G. M. Sheldrick, *Acta Crystallogr., Sect. A* **1990**, *46*, 467–473.

[26] L. J. Farrugia, *J. Appl. Crystallogr.* **1999**, *32*, 837–838.

  

[27] a) G. M. Sheldrick, *SHELXL-97 – Programs for Crystal Structure Analysis*, release 97-2, Göttingen, Germany, **1998**; b) G. M. Sheldrick, *Acta Crystallogr., Sect. A* **2008**, *64*, 112–122.
[28] L. J. Farrugia, *J. Appl. Crystallogr.* **1997**, *30*, 565–566.
[29] C. F. Macrae, P. R. Edgington, P. McCabe, E. Pidcock, G. P. Shields, R. Taylor, M. Towler, J. van de Streek, *J. Appl. Crystallogr.* **2006**, *39*, 453–457.
[30] H. D. Flack, *Acta Crystallogr., Sect. A* **1983**, *39*, 876–881; H. D. Flack, G. Bernardinelli, *Acta Crystallogr., Sect. A* **1999**, *55*, 908–915; H. D. Flack, G. Bernardinelli, *J. Appl. Crystallogr.* **2000**, *33*, 1143–1148; R. Herbst-Irmer, G. M. Sheldrick, *Acta Crystallogr., Sect. B* **1998**, *54*, 443–449; H. D. Flack, G. Bernardinelli, *Chirality* **2008**, *20*, 681–690.

Received: May 4, 2011
Published Online: August 12, 2011

  